VOL.107 NO.IR4. DEC. 1981

JOURNAL OF THE IRRIGATION AND DRAINAGE DIVISION

PROCEEDINGS OF
THE AMERICAN SOCIETY
OF CIVIL ENGINEERS

VOL.107 NO.IR4. DEC. 1981

JOURNAL OF THE IRRIGATION AND DRAINAGE DIVISION

PROCEEDINGS OF THE AMERICAN SOCIETY OF CIVIL ENGINEERS

Copyright© 1981 by
American Society
of Civil Engineers
All Rights Reserved
ISSN 0044-7978

Evan R. Allred, Editor
University of Minnesota

AMERICAN SOCIETY OF CIVIL ENGINEERS

BOARD OF DIRECTION

President
James R. Sims

Past President
Irvan F. Mendenhall

President Elect
John H. Wiedeman

Vice Presidents
Lyman R. Gillis — Paul A. Kuhn
Albert A. Grant — William H. Taylor

Directors
Martin G. Abegg — Arthur R. McDaniel
L. G. Byrd — Robert L. Morris
Frederick W. DeWitt — Paul R. Munger
Larry J. Feeser — William R. Neuman
John A. Focht, Jr. — Leonard S. Oberman
Sergio Gonzalez-Karg — John D. Parkhurst
Kenneth D. Hansen — Celestino R. Pennoni
Ronald C. Hirschfield — Robert B. Rhode
Louis M. Laushey — Gerald E. Speitel
Leon D. Luck — Lawrence E. Wilson, Jr.
Richard S. Woodruff

EXECUTIVE OFFICERS

Eugene Zwoyer, *Executive Director*
Julie E. Gibouleau, *Assistant to the Executive Director*
Louis L. Meier, *Washington Counsel/Assistant Secretary*
William H. Wisely, *Executive Director Emeritus*
Michael N. Salgo, *Treasurer*
Elmer B. Isaak, *Assistant Treasurer*

STAFF DIRECTORS

Donald A. Buzzell, *Managing Director for Education and Professional Affairs*
Robert A. Crist, Jr., *Managing Director for Publications and Technical Affairs*
Alexandra Bellow, *Director, Human Resources*
Joseph A. DeFiglia, *Director, Management Information Services*
David Dresia, *Director, Publications Production and Marketing*
Barker D. Herr, *Director, Membership*
Richard A. Jeffers, *Controller*
Carl E. Nelson, *Director, Field Services*
Don P. Reynolds, *Director, Policy, Planning and Public Affairs*
Bruce Rickerson, *Director, Legislative Services*
Albert W. Turchick, *Director, Technical Services*
George K. Wadlin, *Director, Education Services*
R. Lawrence Whipple, *Director, Engineering Management Services*

COMMITTEE ON PUBLICATIONS

William R. Neuman, *Chairman*
Martin G. Abegg — Ronald C. Hirschfield
John A. Focht, Jr. — Paul R. Munger
Lawrence E. Wilson, Jr.

IRRIGATION AND DRAINAGE DIVISION

Executive Committee
Ronald K. Blatchley, *Chairman*
James N. Luthin, *Vice Chairman*
Karl R. Klingelhofer — E. Gordon Kruse
Conrad Keyes, Jr., *Secretary*
Jack J. Coe, *Management Group D Contact Member*

Publications Committee
Evan R. Allred, ***Chairman and Editor***
Richard H. Hawkins — John A. Replogle
Otto Helweg — Stephen B. Smith
Walter Ochs — James R. Wallace
Allan R. Overman — Jerome J. Zovne
James Luthin, *Exec. Comm. Contact Member*

PUBLICATION SERVICES DEPARTMENT

David Dresia, *Director, Publications Production and Marketing*

Technical and Professional Publications

Richard R. Torrens, *Manager*
Chuck Wahrhaftig, *Chief Copy Editor*
Corinne Bernstein, *Copy Editor*
Linda Ellington, *Copy Editor*
Walter Friedman, *Copy Editor*
Richard C. Scheblein, *Draftsman*

Information Services

Melanie G. Edwards, *Editor*

PERMISSION TO PHOTOCOPY JOURNAL PAPERS

Permission to photocopy for personal or internal reference beyond the limits in Sections 107 and 108 of the U.S. Copyright Law is granted by the American Society of Civil Engineers for libraries and other users registered with the Copyright Clearance Center, 21 Congress Street, Salem, Mass. 01970, provided the appropriate fee is paid to the CCC for all articles bearing the CCC code. Requests for special permission or bulk copying should be addressed to the Manager of Technical and Professional Publications, American Society of Civil Engineers.

CONTENTS

Blaney-Criddle Coefficients for Western Turf Grasses
by John Borrelli, Larry O. Pochop, William R. Kneebone, Ian L. Pepper, Robert E. Danielson, William E. Hart, and Victor B. Youngner 333

Soil Percolation Rates from Neutron Probe Measurements
by Ted S. Vinson and Larry Mahar 343

Dimensionless Stream Advance in Sloping Borders
by Theodor Strelkoff and Albert J. Clemmens 361

TECHNICAL NOTES

Proc. Paper 16689

Relative Runoff by Curve Number Nomograph
by Richard J. Heggen 385

The Journal of the Irrigation and Drainage Division (ISSN 0044-7978) is published quarterly by the American Society of Civil Engineers. Publications office is at 345 East 47th Street, New York, N.Y. 10017. Address all ASCE correspondence to the Editorial and General Offices at 345 East 47th Street, New York, N.Y. 10017. Allow six weeks for change of address to become effective. Subscription price to members is $7.50. Nonmember subscriptions available; prices obtainable on request. Second-class postage paid at New York, N.Y. and at additional mailing offices. IR.

POSTMASTER: Send address changes to American Society of Civil Engineers, 345 East 47th Street, New York, NY 10017.

The Society is not responsible for any statement made or opinion expressed in its publications.

Young's Inequality for Three-Dimensional Flows
by Aristides Th. Marinos 388

Relation Between Curve Number and Runoff Coefficient
by Richard H. McCuen and Timothy R. Bondelid 395

Irrigation Practices for Reclaimed Alkali Soils
by V. V. Dhruva Narayana and N. K. Tyagi 400

Delayed Drainage in a Stream Aquifer System
by Shlomo P. Neuman 407

Simple Equations for Hooghoudt Equivalent Depth
by John G. Sakkas and Vassilios Z. Antonopoulos 411

DISCUSSION

Proc. Paper 16685

Expanded Polystyrene Spheres as Evaporation Suppressors, by Tariq A. Mahmoud and Natiq K. Bashi (Sept., 1980).
by A. F. Thoma 417

INFORMATION RETRIEVAL

The key words, abstract, and reference "cards" for each article in this Journal represent part of the ASCE participation in the EJC information retrieval plan. The retrieval data are placed herein so that each can be cut out, placed on a 3 × 5 card and given an accession number for the user's file. The accession number is then entered on key word cards so that the user can subsequently match key words to choose the articles he wishes. Details of this program were given in an August, 1962 article in CIVIL ENGINEERING, reprints of which are available on request to ASCE headquarters.

STATEMENT OF OWNERSHIP

The *Journal of the Irrigation and Drainage Division* is edited and published by the American Society of Civil Engineers, with general business offices at 345 East 47th Street, New York, N.Y. 10017. The Manager of Technical and Professional Publications is Richard R. Torrens.

This Journal is owned wholly by the American Society of Civil Engineers, a nonprofit educational and professional organization with about 78,000 members. There are no individual owners or stockholders.

	Average No. Copies Each Issue During Preceding 12 Months	Single Issue Nearest To Filing Date
Total no. copies printed (net press run)	6,087	5,858
Paid mail circulation	4,503	4,375
Sales through dealers and counter sales	None	None
Free distribution	None	None
Total distribution	4,503	4,375
Left Over (extra for new orders, office use, etc.)	1,584	1,483
Total	6,087	5,858

I certify that the above statements made by me are correct and complete.—Richard R. Torrens, Manager of Technical and Professional Publications.

16749 BLANEY-CRIDDLE COEFFICIENTS FOR TURF GRASSES

KEY WORDS: **Evapotranspiration;** Irrigation; Lysimeters; **Turf grasses;** Water consumption; **Water supply**

ABSTRACT: Evapotranspiration rates were measured for several turf grasses in Arizona, California, Colorado, and Wyoming. These data were used to calibrate the Blaney-Criddle method for estimating evapotranspiration rates. Warm-season grasses used less water than did cool-season grasses when grown in warm climates. However, Kentucky bluegrass did exhibit heat stress that reduced its evapotranspiration rates below what would be expected when soil temperatures exceed 25/DEG C. The data were collected in urban areas and should be representative of city-wide water requirements for turfed areas.

REFERENCE: Borrelli, John (Assoc. Prof. of Agricultural Engrg., P.O. Box 3354 Univ. of Wyoming, Laramie, Wyo. 82071), Pochop, Larry O., Kneebone, William R., Pepper, Ian L., Danielson, Robert E., Hart, William E., and Youngner, Victor B., "Blaney-Criddle Coefficients for Western Turf Grasses," *Journal of the Irrigation and Drainage Division,* ASCE, Vol. 107, No. IR4, **Proc. Paper 16749**, December, 1981, pp. 333-341

16740 SOIL PERCOLATION RATES

KEY WORDS: Field tests; Infiltration (water); Irrigation systems; **Nuclear probes; Percolation tests; Soil moisture;** Subsurface investigations

ABSTRACT: A study was undertaken to investigate the feasibility of using subsurface neutron moisture probes to estimate soil percolation rates. The measurement procedure developed is based upon the subsurface soil moisture content versus time relationship obtained with a subsurface neutron probe in a soil column in which one-dimensional percolation is occurring. The results from ten laboratory percolation tests employing a column of well-graded sand were used to validate the measurement procedure. The proposed procedure appears to be acceptable for homogeneous deposits of well-graded sand. The validity of the procedure for layered soil profiles or shallow groundwater table conditions must be investigated. The procedure proposed is simpler than traditional methods (e.g., lysimetric) to measure percolation rates.

REFERENCE: Vinson, Ted S. (Assoc. Prof. of Civ. Engrg., Oregon State Univ., Corvallis, Oreg. 97331), and Mahar, Larry, "Soil Percolation Rates From Neutron Probe Measurements," *Journal of the Irrigation and Drainage Division,* ASCE, Vol. 107, No. IR4, **Proc. Paper 16740**, December, 1981, pp. 343-359

16747 DIMENSIONLESS STREAM ADVANCE IN SLOPING BORDERS

KEY WORDS: Border irrigation; Graphs; **Hydraulics;** Mathematical models; **Open channel flow; Surface irrigation; Water distribution**

ABSTRACT: The optimum choice of characteristic reference variables used to put the zero-inertia governing equations of continuity and momentum with boundary condition, into dimensionless form is not obvious. The effect of different choices is noted, as are the effects of choosing different formulas for field roughness and infiltration. The choice of normal depth for characteristic dept, a characteristic distance equal to the quotient of normal depth and bottom slope, and characteristic time equal to the time to travel the characteristic distance at normal velocity leads to a useful two-parameter set of dimensionless curves for advance prior to cut off in a border of indefinite length. These are presented for a series of Kostiakov-infiltration-formula dimensionless coefficients and exponents. It proves possible to present virtually all practical field and laboratory combinations of input variables—inflow rate and border slope, Manning roughness, and infiltration—in ten graphs, each spanning 3 log cycles.

REFERENCE: Strelkoff, Theodor (Independent Consultant, 43 Liberty St., San Francisco, Calif.), and Clemmens, Albert J., "Dimensionless Stream Advance in Sloping Borders," *Journal of the Irrigation and Drainage Division,* ASCE, Vol. 107, No. IR4, **Proc. Paper 16747**, December, 1981, pp. 361-382

U.S. Customary-SI Conversion Factors

In accordance with the October, 1970 action of the ASCE Board of Direction, which stated that all publications of the Society should list all measurements in both U.S. Customary and SI (International System) units, the following list contains conversion factors to enable readers to compute the SI unit values of measurements. A complete guide to the SI system and its use has been published by the American Society for Testing and Materials. Copies of this publication (ASTM E-380) can be purchased from ASCE at a price of $3.00 each; orders must be prepaid.

All authors of *Journal* papers are being asked to prepare their papers in this dual-unit format. To provide preliminary assistance to authors, the following list of conversion factors and guides are recommended by the ASCE Committee on Metrication.

To convert	To	Multiply by
inches (in.)	millimeters (mm)	25.4
feet (ft)	meters (m)	0.305
yards (yd)	meters (m)	0.914
miles (miles)	kilometers (km)	1.61
square inches (sq in.)	square millimeters (mm^2)	645
square feet (sq ft)	square meters (m^2)	0.093
square yards (sq yd)	square meters (m^2)	0.836
square miles (sq miles)	square kilometers (km^2)	2.59
acres (acre)	hectares (ha)	0.405
cubic inches (cu in.)	cubic millimeters (mm^3)	16,400
cubic feet (cu ft)	cubic meters (m^3)	0.028
cubic yards (cu yd)	cubic meters (m^3)	0.765
pounds (lb) mass	kilograms (kg)	0.453
tons (ton) mass	kilograms (kg)	907
pound force (lbf)	newtons (N)	4.45
kilogram force (kgf)	newtons (N)	9.81
pounds per square foot (psf)	pascals (Pa)	47.9
pounds per square inch (psi)	kilopascals (kPa)	6.89
U.S. gallons (gal)	liters (L)	3.79
acre-feet (acre-ft)	cubic meters (m^3)	1,233

Blaney-Criddle Coefficients for Western Turf Grasses

By John Borrelli, A. M. ASCE,[1] Larry O. Pochop,[2] William R. Kneebone,[3] Ian L. Pepper,[4] Robert E. Danielson,[5] William E. Hart, M. ASCE,[6] and Victor B. Youngner[7]

Introduction

Studies of the consumptive use of water by various crops are numerous. For example, Jensen (6) provides an extensive review of the status of these studies. It is obvious from this review that nearly all consumptive use studies have dealt with agricultural crops. Very little information has been acquired concerning the water use of turf grass, and information which does exist is generally difficult to locate (8,11,15).

Turf areas are heavy consumers of water and compete for water traditionally used for other purposes. Water applied to turf is obtained from municipal sources and thus is given priority over other uses such as agriculture and industry. Furthermore, most turf areas are thought of as being relatively small plots of land, although there are over 8,100,000 ha of turf in the United States (2). Of these 8,100,000 ha, about 3,000,000 consist of residential lawns (1,3,9).

The consumptive use of plants usually is estimated through the use of various empirical formulas. The formulas generally require some type of local calibration in order to produce reliable results. Very few attempts to calibrate these formulas for turf have been made (12,14). In fact, Quackenbush and Phelan (12) state: "Additional research on consumptive use of lawn grasses is urgently needed . . ." However, since their publication in 1965, only the attempt by Tovey, et al. (14) to calibrate consumptive use formulas has appeared in national

[1]Assoc. Prof. of Agricultural Engrg., P.O. Box 3354, Univ. of Wyoming, Laramie, Wyo. 82071.

[2]Prof. of Agricultural Engrg., Univ. of Wyoming, Laramie, Wyo.

[3]Prof. of Plant Sciences, Univ. of Arizona, Tucson, Ariz.

[4]Asst. Prof. of Soils, Water, and Engrg., Univ. of Arizona, Tucson, Ariz.

[5]Prof. of Agronomy, Colorado State Univ., Ft. Collins, Colo.

[6]Formerly Assoc. Prof. of Agricultural and Chemical Engrg., Colorado State Univ., Ft. Collins, Colo.

[7]Prof. of Plant Sciences, Univ. of California, Riverside, Calif.

Note.—Discussion open until May 1, 1982. To extend the closing date one month, a written request must be filed with the Manager of Technical and Professional Publications, ASCE. Manuscript was submitted for review for possible publication on January 20, 1981. This paper is part of the Journal of the Irrigation and Drainage Division, Proceedings of the American Society of Civil Engineers, ©ASCE, Vol. 107, No. IR4, December, 1981. ISSN 0044-7978/81/0004-0333/$01.00.

publications. Both of these efforts considered grasses which were grown in open agricultural fields rather than in an urban setting.

Data Sources

Measurements of the consumptive use by urban lawns throughout the western U.S. have been gathered and are used herein to calibrate the SCS (13) version

TABLE 1.—Site Descriptions

Location (1)	Latitude (2)	Longitude (3)	Elevation, in meters (4)	Mean annual precipitation, in centimeters (5)	Mean annual temperature, in degrees centigrade (6)	Average frost free period, in days (7)
Laramie, Wyo.	41°19′N	105°41′W	2,195	25.4	4.9	113
Wheatland, Wyo.	42°05′N	104°57′W	1,433	20.5	9.5	133
Fort Collins, Colo.	40°35′N	105°05′W	1,525	36.3	8.9	140
Northglenn, Colo.	39°54′N	104°59′W	1,665	31.2	10.1	155
Tucson, Ariz.	32°13′N	110°56′W	770	27.6	19.2	245
Santa Ana, Calif.	33°45′N	117°42′W	35	32.8	17.2	316

TABLE 2.—Summary of Data Used

Location (1)	Years of data (2)	Grass type (3)
Laramie, Wyo.	1976–1978	Kentucky bluegrass
Wheatland, Wyo.	1976–1978	Kentucky bluegrass
Fort Collins, Colo.	1977–1978	Kentucky bluegrass
Northglenn, Colo.	1977–1978	Kentucky bluegrass
Santa Ana, Calif.	1966–1969	Common bermuda, St. Augustine
Santa Ana, Calif.	1970–1974	Kentucky bluegrass, tall fescue
Tucson, Ariz.	1977–1979	Bermuda, Santa Ana and Tifgreen hybrid Bermudas, tall fescue, Zoysia, St. Augustine

of the Blaney-Criddle formula. Information describing the locations, years of data, and type of grasses is given in Tables 1 and 2. Consumptive use is defined herein as the evapotranspiration rate experienced when water availability is never a limiting factor. The grasses in all cases were clipped turfs.

Measurements in Wyoming and Colorado were taken using small weighable

lysimeters located directly in residential lawns (8). The lysimeters measured 30.5 cm diam by 70 cm deep. They were made from polyvinyl chloride pipe and were surrounded by retaining sleeves made from the same material. Consumptive use was measured weekly by removing and weighing the lysimeters. Water was then added to bring the soil up to near field capacity. Any excess water above field capacity was allowed to drain to a storage reservoir of gravel

TABLE 3.—Mean Monthly Temperatures During Study Period, in degrees centigrade

Month (1)	Laramie (2)	Wheatland (3)	Fort Collins (4)	Northglenn (5)	Tucson (6)	Santa Ana 1966–1969 (7)	Santa Ana 1970–1974 (8)
Jan.	—	—	—	—	10.7	12.9	11.7
Feb.	—	—	—	—	12.2	13.2	12.9
Mar.	—	—	—	—	14.8	14.2	13.0
Apr.	4.3	8.9	—	—	19.5	14.7	14.5
May	8.4	13.3	—	—	22.5	17.5	16.6
June	14.9	19.1	17.9	19.4	29.1	18.9	19.5
July	18.6	22.8	22.6	23.7	30.8	22.3	21.9
Aug.	16.2	19.9	20.1	21.1	29.6	23.6	22.4
Sept.	12.5	16.4	17.7	19.2	27.7	21.9	20.8
Oct.	5.5	9.7	—	8.6	23.2	18.8	18.2
Nov.	—	—	—	4.6	15.8	16.5	14.5
Dec.	—	—	—	1.7	12.2	12.4	11.8

TABLE 4.—Monthly Percentage of Daytime Hours, *p*, of Year

Month (1)	Laramie (2)	Wheatland (3)	Fort Collins (4)	Northglenn (5)	Tucson (6)	Santa Ana (7)
Jan.	—	—	—	—	7.20	7.10
Feb.	—	—	—	—	6.97	6.91
Mar.	—	—	—	—	8.37	8.35
Apr.	8.97	8.99	—	—	8.76	8.80
May	10.09	10.13	—	—	9.62	9.71
June	10.19	10.25	10.13	10.08	9.59	9.71
July	10.31	10.36	10.26	10.21	9.77	9.88
Aug.	9.60	9.62	9.57	9.55	9.27	9.34
Sept.	8.39	8.40	8.39	8.39	8.34	8.35
Oct.	7.71	7.70	—	7.75	7.95	7.90
Nov.	—	—	—	6.73	7.11	7.02
Dec.	—	—	—	6.55	7.05	6.93

at the bottom of the lysimeters. To assure that adequate moisture was always present, water was added during the week as required so that available moisture depletion was never allowed to exceed 35%. The lysimeters were covered by the homeowner during irrigation of the surrounding lawn, thus preventing unwanted water from being applied. Detailed descriptions of the construction and operation of the lysimeters are given by Pochop, et al. (10).

TABLE 5.—Measured Consumptive Use Values

Month (1)	Bluegrass					Bermudagrass Seeded		
	Wyoming[a] (2)	Wyoming[b] (3)	Colorado[c] (4)	Colorado[d] (5)	California (6)	California (7)	Hi[e] (8)	Low[e] (9)
Jan.	—	—	—	—	59	51	63	—
Feb.	—	—	—	—	64	45	63	26
Mar.	—	—	—	—	77	78	111	37
Apr.	58	100	—	—	104	80	162	105
May	114	124	—	—	103	88	203	134
June	165	156	172	156	131	84	191	178
July	183	168	152	190	169	125	177	151
Aug.	134	124	146	153	145	127	170	124
Sept.	93	113	109	136	108	83	141	111
Oct.	59	70	—	80	77	67	147	110
Nov.	—	—	—	37	63	46	76	81
Dec.	—	—	—	20	48	45	43	26

[a]Laramie.
[b]Wheatland.
[c]Fort Collins.
[d]Northglenn.
[e]Tucson, Ariz.

Measurements in Arizona were taken at the University of Arizona Rincon Vista Turfgrass Research Center in Tucson (8). Thirty lysimeter boxes, 1 m square and 0.60 m deep, constructed of 2.5 cm redwood and lined with a double layer of 6 ml plastic, were used. At the bottom center of each box a tube was attached and sealed to allow addition or removal of water from the box as desired. Each box was connected by its tube to a large glass water bottle arranged as a Marriotte siphon. Water losses from the bottle were measured daily. Consumptive use from both "high" and "low" management regimes was measured. The "high" management included more available water by maintaining the water table consistently 10 cm above that for the "low" regime, heavier nitrogen fertilization, and over-seeding of the warm season grasses with annual ryegrass for winter green grass. The ryegrass was seeded in October and was a factor until May. However, it was a negligible factor in November through January. The water tables were maintained at 35 or 40 cm from the soil surface for the "high," and 45 or 50 cm from the soil surface for the "low" regime. Tall fescue and St. Augustine grasses were tested only at the "low" management regime. Thus, they would have used still more water than indicated had it been available.

Measurements in California were taken at the University of California South Coast Field Station in Santa Ana (15). Measurements were obtained from field plots with water applications controlled automatically by controllers activated by tensiometers at 15 and 30 cm depths. The data used herein are from plots having automatic irrigation and when a tensiometer at either 14 or 30 cm reached 40 cb. These were defined as medium tensiometer treatments and probably

of Turf Grasses, in millimeters per month

Tifgreen		Santa Ana		Zoysia		Tall Fescue		St. Augustine	
Hi° (10)	Low° (11)	Hi° (12)	Low° (13)	Hi° (14)	Low° (15)	California (16)	Arizona (17)	California (18)	Arizona (19)
63	—	64	—	73	—	50	62	53	—
53	28	61	27	81	28	63	39	41	32
111	43	108	40	100	37	82	94	73	50
174	102	175	121	173	106	129	190	78	131
204	150	197	154	191	156	105	242	90	175
221	184	226	199	196	216	148	292	84	258
173	141	199	154	158	174	181	248	109	217
159	124	165	144	165	148	152	176	110	195
134	116	132	127	153	140	109	164	78	190
131	112	118	150	139	122	78	155	50	138
89	60	92	53	73	56	64	59	45	67
61	27	45	39	44	36	49	47	43	64

do not totally meet the criteria of unlimited water availability, although water stress should have been minimal.

Method

The data in Tables 3–5 were used to calibrate the SCS (13) version of the Blaney-Criddle formula for monthly estimates of E_{tp}:

$$u = 25.4\, k_t k_c f \quad \ldots\ldots (1)$$

in which u = the consumptive use (or E_{tp}) for the month, in millimeters; k_t = a coefficient related to temperature; k_c = a crop growth stage coefficient for the month; and f = a consumptive use factor. The coefficient k_t is related to temperature by

$$k_t = 0.0311t + 0.240 \quad \ldots\ldots (2)$$

in which t = the mean temperature for the month, in degrees centigrade. The consumptive use factor f is defined as

$$f = \frac{(1.8t + 32)p}{100} \quad \ldots\ldots (3)$$

in which p = the monthly percentage of daytime hours of the year. Calibration of the formula consisted of calculating k_c values (Table 6) for each month using the averages of the measured consumptive use, and temperature data over two

TABLE 6.—Crop Growth

Month (1)	Bluegrass					Bermudagrass Seeded		
	Wyoming[a] (2)	Wyoming[b] (3)	Colorado[c] (4)	Colorado[d] (5)	California (6)	California (7)	Hi[e] (8)	Low[e] (9)
Jan.	—	—	—	—	1.02	0.83	1.17	—
Feb.	—	—	—	—	1.03	0.71	1.07	0.44
Mar.	—	—	—	—	1.02	0.97	1.27	0.42
Apr.	1.72	1.76	—	—	1.16	0.88	1.28	0.83
May	1.89	1.32	—	—	0.89	0.74	1.22	0.81
June	1.47	1.08	1.31	1.08	0.94	0.61	0.81	0.76
July	1.31	0.92	0.85	1.01	1.02	0.75	0.68	0.58
Aug.	1.21	0.87	1.01	1.01	0.90	0.76	0.73	0.53
Sept.	1.27	1.15	1.01	1.15	0.83	0.61	0.74	0.58
Oct.	1.75	1.34	—	1.69	0.73	0.62	1.03	0.77
Nov.	—	—	—	1.40	0.88	0.59	0.95	1.02
Dec.	—	—	—	1.17	0.84	0.77	0.72	0.44

[a] Laramie.
[b] Wheatland.
[c] Fort Collins.
[d] Northglenn.
[e] Tucson, Ariz.

or more seasons. It should be noted that k_c also contains a meteorological component and does not totally represent the crop which, in this case, is grass (6). The purpose of the information presented in Table 1 (Site Descriptions) is to allow the user to select k_c values from Table 6 from locations that most closely approximate their location.

Calibrations of other formulas beside the SCS (13) version of the Blaney-Criddle were considered. The Blaney-Criddle formula, as presented by Criddle et al. (4), has been calibrated using Wyoming data (8). However, the latter formula requires determination of a seasonal consumptive use factor dependent on the length of the growing season. The growing season length generally needs to be estimated, resulting in a small error. Many other formulas exist, but limitations in availability of required climatic data (e.g., solar radiation, wind, humidity, etc.) generally make these formulas impractical for use in many locations. These formulas are of value if short term estimates of consumptive use are desired. However, the present calibrations are concerned only with monthly data and are not meant to be used for detailed irrigation scheduling purposes. Doorenbos and Pruitt (5) have developed a modification of the Blaney-Criddle formula which permits input of other variables, beside temperature and day length, without direct measurements. This method, however, appears to have little advantage where data from throughout a region are available for calibration of the SCS (13) version of the Blaney-Criddle formula.

Results

The potential evapotranspiration data from Wyoming and Colorado represent

Stage Coefficients (k_c)

Tifgreen		Santa Ana		Zoysia		Tall Fescue		St. Augustine	
Hi° (10)	Low° (11)	Hi° (12)	Low° (13)	Hi° (14)	Low° (15)	California (16)	Arizona (17)	California (18)	Arizona (19)
1.17	—	1.19	—	1.36	—	0.86	1.15	0.86	—
0.90	0.47	1.03	0.46	1.37	0.47	1.01	0.66	0.65	0.54
1.27	0.49	1.24	0.46	1.15	0.42	1.08	1.08	0.91	0.57
1.38	0.81	1.39	0.96	1.37	0.84	1.44	1.50	0.86	1.04
1.23	0.90	1.18	0.93	1.15	0.94	0.91	1.45	0.75	1.05
0.94	0.78	0.96	0.85	0.83	0.92	1.06	1.24	0.61	1.10
0.67	0.54	0.77	0.59	0.61	0.67	1.10	0.95	0.65	0.84
0.68	0.53	0.71	0.62	0.71	0.63	0.95	0.76	0.66	0.84
0.70	0.61	0.69	0.67	0.80	0.73	0.83	0.86	0.58	0.99
0.92	0.79	0.82	1.05	0.97	0.85	0.74	1.08	0.47	0.96
1.12	0.75	1.15	0.66	0.91	0.70	0.89	0.74	0.58	0.84
1.02	0.45	0.75	0.65	0.74	0.60	0.86	0.79	0.73	1.07

city-wide averages. Thus, the calibrated k_c will not necessarily estimate the maximum potential evapotranspiration for a particular plot of turf. It was found in the original experiments (8) that the portion of the lawn located on the south, in direct sunlight during most of the daylight hours, will have 10% more E_{tp} than the city-wide average. As expected, that portion of the lawn located in mostly shaded areas had 10% less E_{tp} than the city-wide average.

The data from Arizona and California were collected from plots and are also good estimates of city-wide evapotranspiration rates. The data from Arizona were collected from within a city, while the data from California were collected at an experimental farm adjacent to a large metropolitan area.

It was possible in Arizona and California to grow both cool season grasses (Kentucky bluegrass and tall fescue) and warm season grasses (St. Augustine, Zoysia, Santa Ana and Tifgreen hybrid bermuda, and seeded bermudagrass). At both locations during the warmer part of the year, the cool season grasses had higher evapotranspiration rates than did the warm season grasses. The tall fescue in Tucson, and Kentucky bluegrass in Wheatland decreased their evapotranspiration rates in midsummer due to heat stress. This phenomenon was not noted for tall fescue in California. It was also noted that the warm season grasses could be mildly water stressed without loss of esthetic characteristics. The high management regime (easier access to water) was obtained by maintaining the water table 10 cm closer to the surface. It is doubtful, however, that a turfed area could be irrigated with the precision necessary to maintain a mild water stress.

Summary

Turf grass evapotranspiration data, taken from lysimeter experiments carried out over several years at several locations, are presented. These data have been used to calibrate the SCS (13) version of the Blaney-Criddle method for estimating evapotranspiration. The results should yield reasonably accurate estimates of city-wide water requirements for turfed areas in many locations in the western U.S. The data were developed with the purpose of using them for water supply studies and not for short-term irrigation scheduling procedures.

In warm regions, the data indicate that warm season turf grasses should be used because they consume consideraly less water. In transition regions, where summer soil temperatures exceed 25° C, users should be aware that the cool season grasses will exhibit heat stress that reduces their evapotranspiration rates below what would be expected with the warm temperatures.

Acknowledgment

The work upon which this publication is based was supported in part by funds provided by the Office of Water Research and Technology, U.S. Department of the Interior, under Public Law 88-279, the Water Resources Research Act of 1964, acting through the Wyoming Water Resources Research Institute.

Appendix.—References

1. American Water Works Association, "Operating Data for Water Utilities 1970 and 1965, *American Water Works Association Statistical Report No. 20112,* American Water Works Association, Littleton, Colo., Dec., 1973.
2. Beard, J. B., *Turfgrass, Science and Culture,* Prentice-Hall, Inc., Englewood Cliffs, N.J., 1973.
3. Cotter, D. J., and Croft, P. B., "Water Application Practices and Landscape Attributes Associated with Residential Water Consumption," *Water Resources Research Institute Report No. 049,* New Mexico Water Resources Research Institute, Las Cruces, N.M., Nov., 1974.
4. Criddle, W. D., Harris, K., and Willardson, L. S., "Consumptive Use and Water Requirements for Utah," *Technical Bulletin No. 8 (Rev.),* Office of the State Engineer, State of Utah, 1962.
5. Doorenbos, J., and Pruitt, W. O., "Guidelines for Predicting Crop Water Requirements," *Food & Agricultural Organization of the United Nations Irrigation and Drainage Paper No. 24,* Food and Agriculture Organization of the United Nations, Rome, 1977.
6. Jensen, M. E., ed., "Consumptive Use of Water and Irrigation Water Requirements," a report prepared by the Technical Committee on Irrigation Water Requirements of the Irrigation Drainage Division of ASCE, 1973.
7. Kneebone, W. R., "Water Use by Grasses," *Proceedings Arizona Turfgrass Conference,* Tucson, Ariz., 1979, pp. 5–8.
8. Kneebone, W. R., et al., "Water Requirements for Urban Lawns," *Project Completion Report to Office of Water Research & Technology Project B-035-WYO,* Wyoming Water Resources Research Institute, Laramie, Wyo., Sept., 1979.
9. Linaweaver, F. P., et al., "A Study of Residential Water Use," *Federal Housing Administration Technical Studies Program,* U.S. Government Printing Office, Washington, D.C., 1967.
10. Pochop, L. O., et al., "Water Requirements and Application Rates for Lawns," *Water Resources Series No. 71,* Wyoming Water Resources Research Institute, Laramie, Wyo., Feb., 1978.
11. Pochop, L. O., and Borrelli, J., "Water Use by Kentucky Bluegrass," *Proceedings*

Arizona Turfgrass Conference, Tucson, Ariz., 1979, pp. 18–20.
12. Quackenbush, T. H., and Phelan, J. T., "Irrigation Water Requirements of Lawns," *Journal of the Irrigation and Drainage Division,* ASCE, Vol. 91, No. IR2, Apr., 1965, pp. 11–19.
13. Soil Conservation Service, "Irrigation Water Requirements," *Technical Release No. 21,* USDA-Soil Conservation Service, Engineering Division, 1967.
14. Tovey, R., Spencer, J. S., and Muckel, D. C., "Water Requirements of Lawn Grass," *Transactions of the American Society of Agricultural Engineers,* Vol. 12, No. 3, June, 1969, pp. 356–358.
15. Youngner, V. B., "Turfgrass Water Use—University of California Studies," *Proceedings Arizona Turfgrass Conference,* Tucson, Ariz., 1979, pp. 8–17.

Soil Percolation Rates from Neutron Probe Measurements

By Ted S. Vinson,[1] M. ASCE and Larry Mahar,[2] A. M. ASCE

Introduction

The design of irrigation systems and facilities to dispose of wastewater generally requires knowledge of soil percolation rates at a given site. In the past, soil percolation rates have been established with lysimeters (3,12,15,20,21,31). Three types of lysimeters, and their characteristics, are identified in Table 1, namely: (1) Soil block; (2) filled-in; and (3) unconfined. Lysimeters, however, have many disadvantages when they are used to determine percolation rates. Soil block and filled-in lysimeters, physically confine runoff which results in unnatural ponding at the surface. For a filled-in lysimeter the disturbance associated with the removal and replacement of the soil obviously has a significant influence on the percolation rate measured. If an air-water interface is present, as is the case with many unconfined lysimeters, gravitational forces must overcome capillary tension forces before percolate can leave the soil. A vacuum may be applied through the lysimeter, but only percolate held by capillary tension equal to or less than atmospheric pressure will be removed. With the unconfined lysimeter the lack of side walls precludes a definition of the soil block from which the percolate is collected. Further, if the soil is dry, water may flow around the unconfined lysimeter; if it is wet, the lysimeter may function as a drain for the surrounding soil mass. Finally, the mere presence of a lysimeter and its location and method of removing percolate can cause modifications in the natural soil moisture-tension profile and, hence, percolation characteristics. Several modified moisture-tension profiles which illustrate this problem are shown in Fig. 1.

In recognition of the limitations associated with the use of lysimeters to measure quantities of soil percolate and percolation rates, and as part of a long-term project to establish hydrologic conditions at a spray irrigation facility (30), a study was undertaken to investigate the feasibility of using subsurface neutron moisture probes to estimate soil percolation rates. The results from the study are reported herein.

[1]Assoc. Prof. of Civ. Engrg., Oregon State Univ., Corvallis, Oreg. 97331.
[2]Staff Engr., ERTEC-Western, Long Beach, Calif.

Note.—Discussion open until May 1, 1982. To extend the closing date one month, a written request must be filed with the Manager of Technical and Professional Publications, ASCE. Manuscript was submitted for review for possible publication on May 6, 1981. This paper is part of the Journal of the Irrigation and Drainage Division, Proceedings of the American Society of Civil Engineers, ©ASCE, Vol. 107, No. IR4, December, 1981. ISSN 0044-7978/81/0004-0343/$01.00.

TABLE 1.—Types and Characteristics of Lysimeters

Type (1)	Characteristics (2)
Soil block (monolith or undisturbed)	Confining side walls built around an essentially undisturbed block of soil; partly open bottom is installed through which percolate is collected.
Filled-in	Container with vertical walls, an open top, and an open bottom through which percolate is collected; it is filled with soil that has been removed from its original location and recompacted to the in-situ condition.
Unconfined	Percolate passing through in-situ undisturbed soil is collected in a funnel or pan placed under the soil and then conveyed to the surface through a tube.

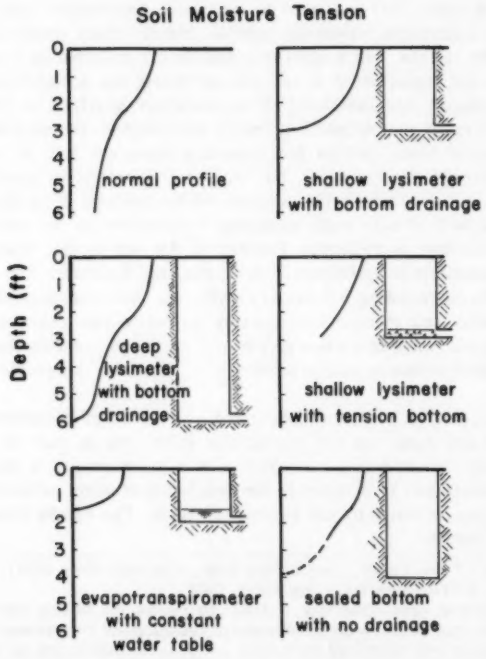

FIG. 1.—Soil Moisture Tension Versus Depth for Several Types of Lysimeters Under Identical Conditions Few Days After Precipitation (after Pelton, 1961)

Use of Neutron Probe for Subsurface Soil Moisture Determination

The development of nuclear devices to measure in situ soil properties dates back to 1941 when Pontecorvo (22) published a paper describing a device to detect fluid bearing zones for petroleum exploration. Considerable research was conducted on the measurement of soil moisture and density by nuclear methods during the 1950s and 1960s (2,4,5,7,8,9,10,11,13,16,17,18,23,24,25,26,27,28) which resulted in increased confidence in the use of nuclear devices. Recently, subsurface nuclear probes have been used to determine in situ moisture around drilled shafts (6), downward movement of water resulting from natural precipitation (14), the measurement of in situ soil moisture and density in a tailings dam (19), and changes in subgrade moisture under a roadbed (29).

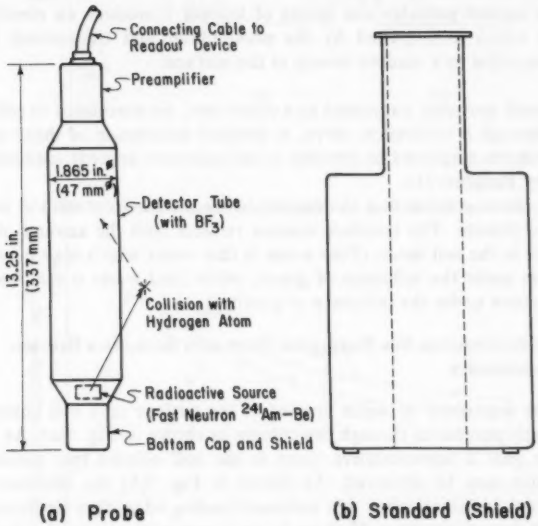

FIG. 2.—Subsurface Neutron Moisture Probe

The present configuration of a subsurface nuclear probe, specifically a neutron probe, is shown in Fig 2. The probe consists of a bottom cap and shield, radioactive source, detector tube, and preamplifier. The probe is used in conjunction with a standard. The standard has a dual purpose in that it provides the reference count used in the calibration procedure for the probe to arrive at soil moisture content and it acts as a shield against radiation exposure.

To obtain subsurface readings, the probe is lowered into the ground through an access (monitoring) tube. The access tube is usually thin-walled aluminum irrigation tubing or steel pipe whose diameter is slightly larger than the diameter of the probe. A close fit between the access tube and the probe is essential to obtain accurate results. To eliminate direct contact with the radioactive source,

the probe, located inside the standard, is placed on top of the access tube and then lowered down the tube.

The following events occur in the determination of soil moisture content with the neutron probe (refer to Fig. 2):

1. The depth moisture probe emits fast neutrons from a 241 Am-Be source radially into the strata.
2. The fast neutrons are slowed down as a result of elastic collisions with the hydrogen atoms in the strata.
3. Some of the slowed (thermal) neutrons are backscattered toward the detector region of the probe and are absorbed by the boron trifluoride (BF_3). Highly ionized alpha particles and atoms of lithium 7 are produced upon the absorption of the slow neutrons by the BF_3.
4. The ionized particles and atoms of lithium 7 produce an electrical pulse or signal which is amplified by the preamplifier and transmitted through a connecting cable to a readout device at the surface.

The detected neutrons, expressed as a count rate, are correlated to soil moisture content through a calibration curve. A detailed description of these events and the procedures employed to develop a soil moisture content calibration curve is given by Bruggers (1).

The moisture content that is determined by the neutron method is reported in units of density. The moisture content reflects both the amount of free and held water in the soil mass. (Free water is that water which may move through a soil mass under the influence of gravity while held water is that water which does not move under the influence of gravity.)

Procedure for Estimating Soil Percolation Rates from Subsurface Neutron Probe Measurements

Consider a quantity of water applied at the surface of a soil column which subsequently percolates through the column as shown in Fig. 3(*a*). As the water percolates past a representative point in the soil column two timedependent relationships may be observed. As shown in Fig. 3(*b*) the moisture content, starting from an initial value, will increase (leading edge) then decrease (trailing edge) with increasing time. If there is no increase in storage in the soil, the moisture content will return to its initial value. As shown in Fig. 3(*c*) the velocity, starting at zero, also increases and decreases with increasing time, eventually returning to zero. Referring to Fig. 3(*b*), it is noted that at any time t, the amount of water moving through the soil column may be assumed to be equal to the change in moisture content of the soil column, that is, Δmc_t. The amount of water in the soil column is moving at a velocity V_t as noted in Fig. 3(*c*). By inspection, the percolation rate at time t, PR_t, may be calculated from

$$PR_t = \frac{(\Delta mc_t)(V_t)}{\gamma_w} \quad \ldots\ldots\ldots\ldots\ldots\ldots\ldots\ldots\ldots\ldots\ldots\ldots\ldots\ldots\ldots\ldots (1)$$

in which, γ_w = density of water.

To determine percolation rates employing Eq. 1 it is, therefore, necessary to determine the moisture content and velocity relationship with time at a given

point in a soil column. In practice, it is possible to determine the moisture content versus time relationship at a given point with a subsurface neutron probe, but it is not possible to determine the velocity versus time relationship at a given point. However, the velocity versus time relationship can be determined over a representative volume of material as follows:

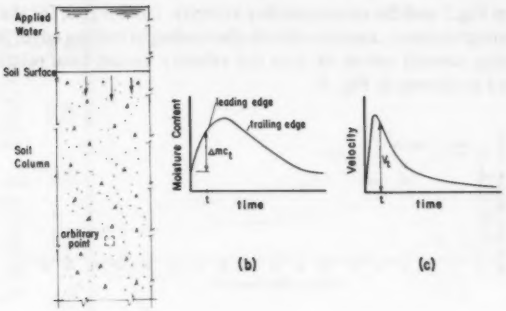

FIG. 3.—One Dimensional Percolation in Soil Column

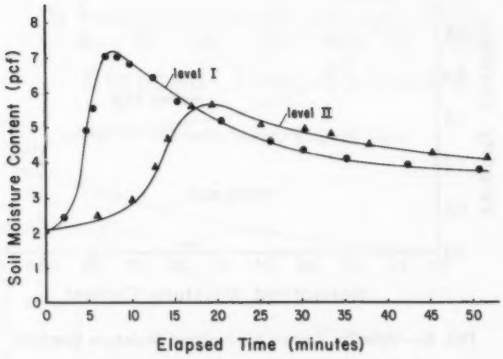

FIG. 4.—Soil Moisture Content Versus Elapsed Time at Two Levels

1. Determine the soil moisture content versus time relationship at two levels, I and II, in a soil column separated by a distance L (refer to Fig. 4).
2. Divide the ordinate values of moisture content by the respective peak moisture contents obtained at the two levels; the result is two normalized moisture content versus time relationships of approximately the same shape but with peak values at different times.
3. Superimpose the two normalized moisture content versus time relationships as shown in Fig. 5.

4. Calculate the velocity of the water as a function of normalized moisture content by noting the elapsed time between equal normalized moisture contents on the leading and trailing edge, respectively, of level I and II and dividing the distance between the levels, L, by the elapsed time; the result is the relationship shown in Fig. 6.

5. For either level I or II at a time t determine the normalized moisture content from Fig. 5 and the corresponding velocity, from Fig. 6, for the normalized moisture content at time t, associated with the leading or trailing edge, respectively. By considering several values of time the velocity versus time relationship may be developed as shown in Fig. 7.

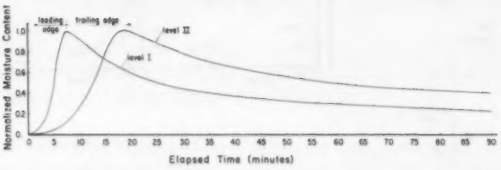

FIG. 5.—Superimposed Normalized Moisture Contant Versus Elapsed Time at Two Levels

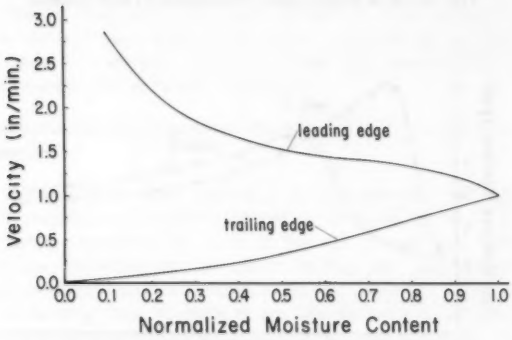

FIG. 6.—Velocity Versus Normalized Moisture Content

The validity of the approach outlined above is based primarily on the assumption that the velocity of the water can be determined from a knowledge of the elapsed time between equal normalized moisture contents. To the authors' knowledge there is no precedent for this assumption for unsaturated flow. For saturated flow with no changes in soil fabric during flow, Darcy's Law provides validity for the procedure. Specifically, Darcy's Law may be written

$$V = k \cdot \frac{dH}{dz} \quad \ldots \ldots \ldots

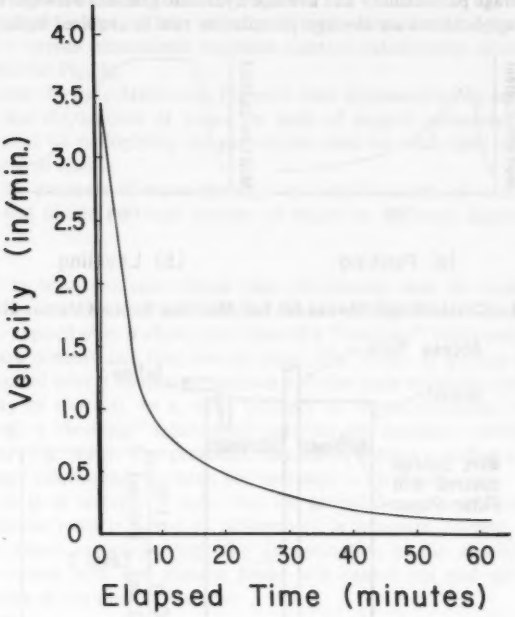

FIG. 7.—Velocity Versus Elapsed Time

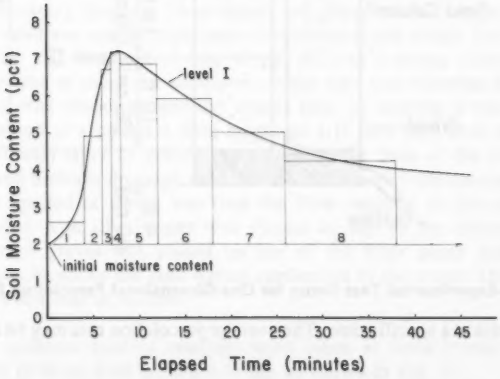

FIG. 8.—Incremental Soil Moisture Content Versus Elapsed Time

The assumption stated would mean the calculated velocity is simply associated with the average permeability and average hydraulic gradient between two levels.

In many applications an average percolation rate is required rather than the

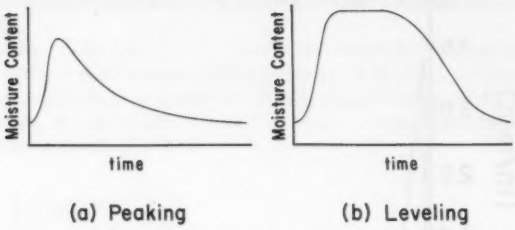

FIG. 9.—Characteristic Shapes for Soil Moisture Content Versus Time

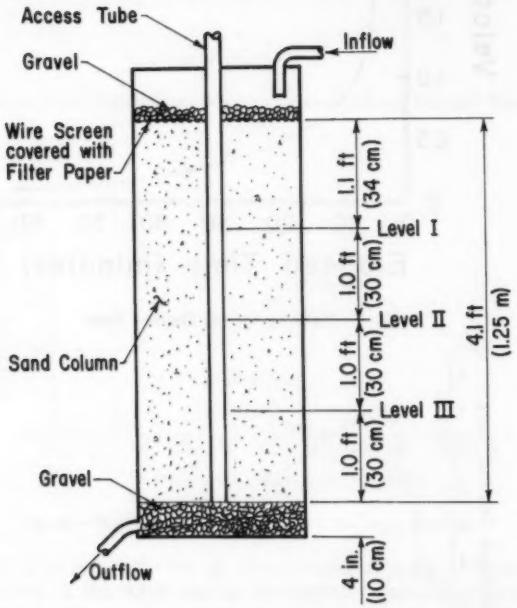

FIG. 10.—Experimental Test Setup for One-Dimensional Percolation Study

percolation rate at a specific time. The average percolation rate may be determined as follows:

1. Divide the moisture content versus time curve at level I or II into increments of time as shown in Fig. 8; the increments should be smaller in the nonlinear regions; they can be larger in the linear regions.

2. For each time increment estimate the average change in moisture content and the average normalized moisture content.

3. Estimate the average flow velocity of each element with a knowledge of the velocity versus normalized moisture content relationship determined for the test (refer to Fig. 6).

4. Calculate the percolation rate for each time increment using equation (1).

5. Calculate the amount of water (in units of length) associated with each time increment by multiplying the percolation rate for each time increment by the increment of time.

6. Sum the amounts of water (in units of length) associated with each time increment and divide the total amount of water by the total elapsed time for the event.

The soil moisture content versus time relationship may be represented by either of the two characteristic shapes shown in Fig. 9. If a small quantity of water is applied over a short time interval a "peaking" relationship between soil moisture content and time results [Ref. Fig. 9(*a*)]. If a large quantity of water is applied over a short time interval and the peak moisture content equals the capacity of the soil, or a small quantity of water is applied over a long time interval, a "leveling" relationship between soil moisture content and time results [Ref. Fig. 9(*b*)]. The procedure presented applies to either a "peaking" or "leveling" relationship between soil moisture content and time.

Finally, it is of interest to note that the procedure presented to determine soil percolation rates is based on differences in moisture content. Therefore, systematic errors associated with the determination of the absolute value of moisture content with the neutron probe will cancel out and not affect the determination of the percolation rate.

Laboratory Program to Evaluate Soil Percolation Rates

In the laboratory program to evaluate soil percolation rates a column of well-graded sand was used to represent a one-dimensional model. The test setup, shown in Fig. 10, consisted of two 55 gal (0.21 m^3) drums containing a 4.1 ft (1.3 m) column of sand. An aluminum access tube was centered in the drums and the sand was placed around the access tube by pouring it through a #30 sieve maintained at a constant drop height of 1 ft (300 mm) over the surface. A 4 in. (100 mm) layer of gravel was placed at the base of the column. The gravel allowed uniform drainage over the cross section of the column. To allow water to be applied at a rate less than the flow capacity of the sand, a wire screen covered with filter paper was placed on top of the column. Finally, a thin layer of gravel was placed on top of the filter paper and screen to minimize disturbance of the sand during application of the water. The procedure to conduct a test was as follows:

1. Initial moisture content readings were taken at three levels: 1.1 ft, 2.1 ft, and 3.1 ft (0.35 m, 0.66 m, and 0.97 m), as shown in Fig. 10.

2. With the subsurface neutron probe at level I, water was applied at a constant head until the total amount of water associated with the test had been added. The water level was then allowed to fall.

TABLE 2.—Example Calculation of Percolation Rates

Change in Moisture Content, in pounds per cubic foot		Normalized change in moisture content	Elapsed Time between Equal Normalized Moisture Contents, in minutes		Velocity, in inches per minute		Time at Level I, in minutes		Percolation Rate, in inches per minute	
Level I (1)	Level II (2)	(3)	Leading edge (4)	Trailing edge (5)	Leading edge (6)	Trailing edge (7)	Leading edge (8)	Trailing edge (9)	Leading edge (10)	Trailing edge (11)
0.52	0.37	0.1	4.21	240	2.85	0.05	2.6	—	0.024	0.0004
1.04	0.74	0.2	5.45	109	2.20	0.11	3.6	—	0.037	0.002
1.56	1.11	0.3	6.42	75	1.87	0.16	4.2	62	0.047	0.004
2.08	1.48	0.4	7.10	54.5	1.69	0.22	4.6	34.5	0.056	0.007
2.60	1.85	0.5	7.74	37.5	1.55	0.32	5	24.5	0.065	0.013
3.12	2.22	0.6	8.22	28.6	1.46	0.42	5.3	20.0	0.073	0.021
3.64	2.59	0.7	8.57	20.0	1.40	0.60	5.6	15.6	0.082	0.035
4.16	2.96	0.8	8.82	16.0	1.36	0.75	6.0	13.8	0.091	0.050
4.68	3.33	0.9	9.60	13.48	1.25	0.89	6.5	10.5	0.094	0.067
5.20	3.70	1.0	11.43	11.43	1.05	1.05	7.4	7.4	0.088	0.088

Note: 1 lb = 0.453 kg; 1 cu ft = 0.028 in.^{3}; 1 in. = 25.4 mm.

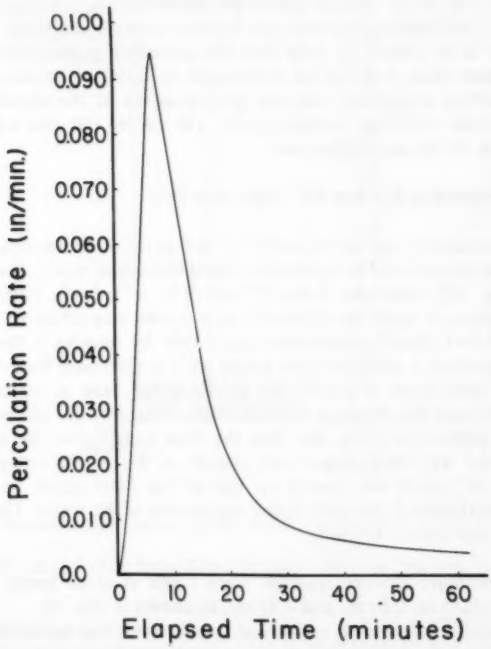

FIG. 11.—Percolation Rate Versus Elapsed Time

3. A timer was started at the instant the water was applied and moisture content readings were taken every 15 sec at level I. When an increase in moisture content was observed the probe was lowered to level II and readings were taken at 15 sec intervals. When an increase was observed at level II the probe was moved back to level I where another 15 sec reading was taken. Thereafter the probe was moved consecutively to all three levels at 15 sec intervals and readings were taken.

4. Readings were taken until either the count ratio was equal to the initial reading or until the moisture content versus time curve became linear.

5. The percolate was collected at the base of the column and weighed.

The data obtained from the test can be represented on a plot of moisture content versus time for each of the three levels. The data was analyzed to estimate the percolation rate versus time relationship using the procedures discussed in the preceding section. An example calculation is given in Table 2 for the event shown in Fig. 4 as recorded for levels I and II. Figs. 5, 6, and 7 support the example calculation presented. A summary of the test results, the percolation rate versus time relationship, is shown on Fig. 11.

Analysis of Test Results

The validity of the proposed procedure to determine percolation rates was assessed by calculating the total amount of percolate for a given test and comparing

TABLE 3.—Example Calculation of Amount of Water Percolating Through Soil Column

Element number (1)	Increment of time in minutes (2)	Average change in moisture content, in pounds per cubic foot (3)	Average normalized moisture content (4)	Velocity, in inches per minute (5)	Percolation rate, in inches per minute (6)	Amount of water, in pounds (7)
1	4	.6	.11	3.0	0.29	1.9
2	2	2.9	.56	1.5	.70	2.3
3	1	4.7	.90	1.25	.94	1.5
4	1	5.2	1.00	1.00	.083	1.4
5	4	4.8	.92	.90	.070	4.6
6	6	3.9	.75	.65	.040	3.9
7	8	3.0	.57	.35	.017	2.2
8	12	2.2	.42	.25	.009	1.8
9	95	1.0	.19	.10	.002	3.1
						Total = 22.7 lb
						Actual = 22.0 lb

Note: Cross-sectional area of drum = 452 in.^{2}; 1 lb = 0.453 kg; 1 cu ft = 0.028 m^3; 1 in. = 25.4 mm.

it to the amount collected. The calculation of the amount of percolate requires the use of the percolation rates. Therefore, a favorable comparison between the amount of percolate calculated to that collected would substantiate the intermediate calculation of the percolation rate. The total amount of percolate may be determined by the procedure given in a preceding section to estimate the average percolation rate. A deviation to the procedure is required in the last step as follows:

1. Sum the amounts of water (in units of length) associated with each time increment and multiply by the cross-sectional area of the drum and the density of water.

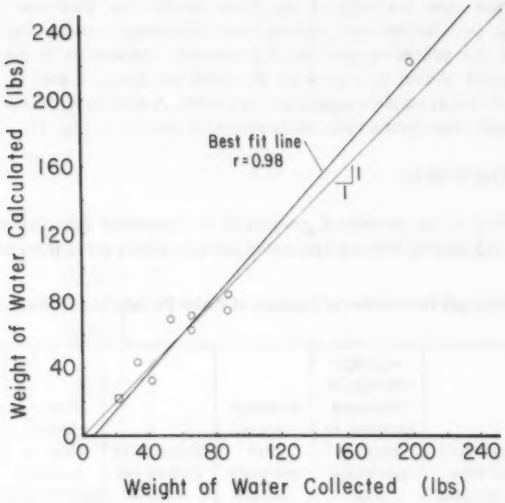

FIG. 12.—Weight of Water Calculated Versus Weight of Water Collected at Level II-III

An example calculation is given in Table 3 for the test results presented in Fig. 4. Fig. 6 supports the example calculation presented.

A total of 10 laboratory tests were conducted with the amount of water applied ranging from 10 lb–100 lb (4.5 kg–90 kg). The percolation rates and total amount of percolate were determined for each test using the data from levels I and II, II and III, and I and III. Fig. 12 shows the comparison between the total amount of percolate calculated using the data from levels II and III and total amount collected. (Note: Level III measurements are missing for one of the tests, thus, only nine data points are shown.) The least squares best fit line for the data set, with a correlation coefficient of 0.98 is also shown. The slope of the regression line is close to the 1:1 line and suggests that the estimated

percolation rates are very reasonable compared to the measured values.

Fig. 13 shows the comparison between the total amount of percolate calculated using the data from levels I and II and I and III. The least squares best fit lines for the data sets, with correlation coefficients of 0.96 (level I and II) and 0.98 (level I and III) are also shown. The comparisons are not as favorable as that shown in Fig. 12. The relationship obtained in Fig. 13 may be explained by considering the sphere of influence of the neutron probe. van Bavel, et al. (28) determined an approximate relationship for the radius, r, of the sphere of influence as follows:

$$r = 5.9 \left(\frac{100}{\text{moisture content in percent by volume}} \right)^{1/3} \quad \ldots\ldots\ldots\ldots (3)$$

For the tests conducted the radius of the sphere of influence is between 18 in. (460 mm) at low moisture contents and 9 in. (230 mm) at high moisture contents. Therefore, at the low moisture contents associated with the start of a test, for the level I readings, the radius of influence would extend above the top of the soil column. When the water reservoir was created above the soil column to conduct a test, the zone of influence would extend into the reservoir and result in higher moisture content readings than exist in the soil. Calculated percolation rates based on level I data would, therefore, be higher than actually occurred. Also calculated weights of percolate water would be greater than the amounts of percolate water collected as shown in Fig. 13.

Determination of In Situ Percolation Rates

The procedure to estimate soil percolation rates with subsurface neutron probes was presented in a preceding section. The procedure applies to the determination of percolation rates for both laboratory and field conditions. The procedure employed to determine soil percolation rates in situ will differ from the procedure employed in the laboratory in two aspects, namely: (1) The installation of the access tube; and (2) the time increments at which moisture content readings are taken.

Installation of the access tube should satisfy three requirements (29):

1. There should be a snug fit between the access tube and surrounding soil.
2. The access tube should be watertight to prevent water and moisture from entering.
3. The access tube should be straight and circular to allow passage of the probe.

At least three methods are commonly employed to meet these requirements as follows:

1. Driving the access tube closed-end by means of a drop hammer (applicable only to very soft soil deposits).
2. Driving an open-end access tube and removing the material from inside the tube with an auger.

3. Pre-augering a hold and driving the access tube closed-end into the hole.

It would appear that any one of these three techniques would be suitable.

The time increment at which moisture content readings are taken will depend to a great degree on the soil conditions at a given site. Fig. 14 shows the

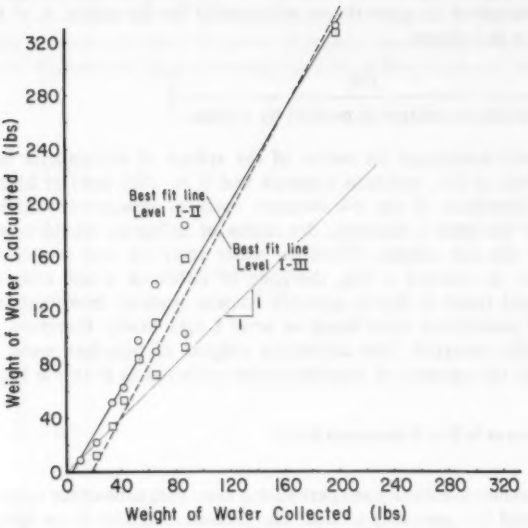

FIG. 13.—Weight of Water Calculated Versus Weight of Water Collected at Levels I-II and I-III

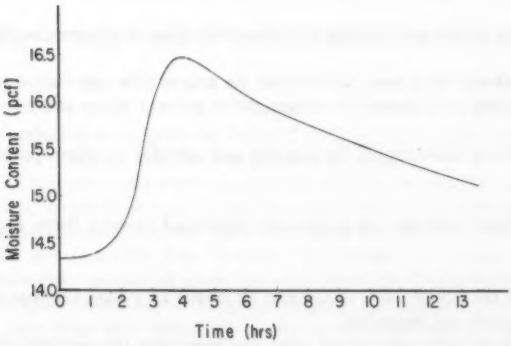

FIG. 14.—Soil Moisture Content Versus Time at Field Test Site

moisture content versus time relationship obtained at a level of 2 ft (0.6 m) following the spray application at a spray irrigation facility. The soils at the site consist of silty fine to medium glacial outwash sand overlain by a 3 in. (80 mm) layer of organic topsoil and vegetal cover. The time scale for the moisture content relationship for the materials at the site is in hours, owing to the relatively low permeability of the soils at the site. Moisture content readings were taken at 20 min intervals. Further, a considerable time period was required to obtain the complete moisture content relationship at this particular site.

The results from the laboratory test program suggest that moisture content readings should not be taken close to the surface of the soil deposit and the distance between the levels at which readings are taken should be 1 ft (0.31 m) or less. Additional research work is needed to more accurately define appropriate distances from the surface and between successive levels as a function of soil type and moisture content.

van Bavel, et al. (28) suggest that the neutron probe can be lowered into an access tube and the density of detected neutrons, expressed as a count rate, can be observed as a function of depth. The count rate will increase with depth until the soil-air boundary is outside the sphere of influence of the probe. At this depth the count rate will level off and the readings are associated with an "infinite" body. This concept could easily be applied to a field situation to determine the minimium reading depth.

Finally, the conclusions drawn in the paper are associated with a moist homogeneous column of well-graded sand. In the field layered soil profiles (in which the materials have significantly different permeabilities) or shallow ground-water table conditions can exist. The validity of the proposed procedure under these conditions is questionable and requires further evaluation.

Summary and Conclusions

A procedure is presented to estimate soil percolation rates with subsurface neutron probes. The procedure is based upon the soil moisture content versus time relationship obtained at two levels in a soil column or soil profile in which one-dimensional percolation is occurring. The results from 10 laboratory tests employing a column of well-graded sand in which percolation was occurring were used to validate the procedure. The calculated quantities of water for the 10 percolation tests compared favorably to the actual amount of water collected. Therefore, the procedure proposed appears to be acceptable for homogeneous deposits of well-graded sand. The validity of the procedure for layered soil profiles or shallow ground-water table conditions must be investigated. The procedure proposed is simpler than traditional methods (e.g., lysimetric) to measure percolation rates.

When using subsurface neutron probes to estimate percolation rates in situ, consideration must be given to the method of installation of the access tube, the time intervals at which moisture contents will be determined at a particular site, the depth from the ground surface to the level where moisture content readings are taken, and the distance between levels where moisture content readings are taken.

Acknowledgment

The studies described in this paper were supported in part by the U.S. Environmental Protection Agency under Grant No. R 00514301 and in part by the Office of Water Research and Technology, U.S. Department of Interior, under Annual Allotment Project A-079-MICH. The support of these agencies is gratefully acknowledged. D. C. Wiggert and D. McIntosh offered many helpful suggestions during the course of the studies.

Appendix I.—References

1. Bruggers, D. E., "Determination of In Situ Soil Properties with Subsurface Nuclear Probes," thesis presented to Michigan State University, at East Lansing, Mich., in 1976, in partial fulfillment of the requirements for the degree of Master of Science.
2. Burn, K. N., "Design and Calibration of a Neutron Moisture Meter," *ASTM Special Technical Publication No. 293*, Symposium on Nuclear Methods for Measuring Soil Density and Moisture, June 27, 1960.
3. Davison, B. E., "The Relationship of Temperature and Ice to Infiltration at a Spray Irrigation Facility," thesis presented to Michigan State University, at East Lansing, Mich., in 1975, in partial fulfillment of the requirements for the degree of Master of Science.
4. DeBoodt, M., Hartman, R., and DeMeester, P., "Determination of Soil Moisture Characteristics for Irrigation Purposes by Neutron Moisture Meters and Air Purge Tensiometers," presented at the June, 1967, *Symposium on Isotope and Radiation Techniques in Soil Physics and Irrigation Studies*, held at Istanbul, Turkey, pp. 147–158.
5. Douglas, J. E., "Volumetric Calibration of Neutron Moisture Probes," *Soil Science Society American Proceedings*, Vol. 30, 1966, pp. 541–544.
6. Ehlers, C. J., Reese, L. C., and Anagnos, J. N., "The Nuclear Method of Soil Moisture Determination at Depth," *Report No. 89-4*, University of Texas at Austin, Austin, Tex., June, 1969.
7. Gardner, R. P., and Roberts, K. F., "Density and Moisture Content Measurements by Nuclear Methods," *National Cooperative Highway Research Program Rept. 43*, Final Report, 1967.
8. Gardner, W. H., and Calissendorff, "Gamma Ray and Neutron Attenuation in Measurement of Solid Bulk Density and Water Content," presented at the June, 1967, *Symposium on Isotope and Radiation Techniques in Soil Physics and Irrigation Studies*, held at Istanbul, Turkey, pp. 101–111.
9. Gardner, W. R. and Kirkham, D., "Determination of Soil Moisture by Neutron Scattering," *Soil Science*, Vol. 73, No. 5, 1952, pp. 391–401.
10. Gurr, C. G., "Use of Gamma Rays in Measuring Water Content and Permeability in Unsaturated Columns of Soil," *Soil Science*, Vol. 94, July–December, 1962, p. 224.
11. Jenson, P. A., and Somer, E., "Scintillation Techniques in Soil-Moisture and Density Measurements," presented at the June, 1967, *Symposium on Isotope and Radiation Techniques in Soil Physics and Irrigation Studies*, held at Istanbul, Turkey, pp. 31–45.
12. King, K. M., Tanner, C. B., and Suomi, V. E., "A Floating Lysimeter and its Evaporation Recorder," *Transactions American Geophysical Union*, 1959, 37(6):738–742.
13. King, L. G., "Gamma-ray Attenuation for Soil-Water-Content Measurements Using 241 Am," presented at the June, 1967, *Symposium on Isotope and Radiation Techniques in Soil Physics and Irrigation Studies*, held at Istanbul, Turkey, pp. 17–28.
14. Klute, A., Danielson, R. E., Linden, D. R., and Hamaker, P., "Groundwater Recharge as Affected by Surface Vegetation and Management," Research Report, Department of Agronomy, Colorado State University, Dec., 1972.
15. Kohnke, H., Dreibelbis, F. R., and Davidson, J. M., "A Survey and Discussion of Lysimeters and a Bibliography on Their Construction and Performance," *Misc. Pub. 372*, U.S. Department of Agriculture, Washington, D.C., May, 1940.

16. LeFevre, E. W., and Manke, P. G., "A Tentative Calibration Procedure for Nuclear Depth Moisture/Density Gauges," National Research Council, Highway Research Record, Vol. 248, 1968.
17. Marais, P. G., and Smit, W. B., "Laboratory Calibration of the Neutron Moisture Meter," *South African Journal of Agricultural Science,* Johannesburg, South Africa, Vol. 3, No. 4, Dec., 1960, p. 581.
18. McHenry, J. R., and Gill, A. C., "The Influence of Bulk Density, Slow Neutron Absorbers, and the Time on the Calibration of Neutron-Moisture Probes," presented at the June, 1967, *Symposium on Isotope and Radiation Techniques in Soil Physics and Irrigation Studies,* held at Istanbul, Turkey, pp. 83–97.
19. Mittal, H. K., and Morgenstern, N. R., "Parameters for the Design of Tailing Dams," Research Report, Department of Civil Engineering, University of Alberta, Edmonton, Alberta, 1973.
20. Parizek, R. R., and Lane, B. E., "Soil-Water Sampling Using Pan and Deep Pressure-Vacuum Lysimeters," *Journal of Hydrology,* Vol. 11, North-Holland Publishing Co., Amsterdam, The Netherlands, 1970, pp. 1–21.
21. Pelton, W. C., "The Use of Lysimetric Methods to Measure Evapo-transpiration," *Proceedings of Hydrology Symposium No. 2, Evaporation,* Queens Printer, Ottawa, Canada, 1961, pp. 106–127.
22. Pontecorvo, B., "Neutron Well Logging," *Oil and Gas Journal,* Sept., 1941, p. 32.
23. Stone, J. F., "Statistical Parameters and Reproducibility of the Neutron Method of Measuring Soil Moisture," *Proceedings,* Soil Science Society of America, Vol. 24, 1960, pp. 435–438.
24. Troxler, W. F., "Calibration of Nuclear Meters for Measuring Moisture and Density," Symposium on Soil Mechanics, *ASTM Special Technical Publication No. 351,* 1963, pp. 29–41.
25. van Bavel, C. H. M., Stirk, G. B., "Soil Water Measurement with an AM 241-Be Neutron Source and an Application to Evaporimetry," *Journal of Hydrology,* Vol. 5, Amsterdam, The Netherlands, 1967, p. 4046.
26. van Bavel, C. H. M., "Calibration and Characteristics of Two Neutron Moisture Probes," *Proceedings, Soil Science Society of America,* Vol. 25, 1961, pp. 329–334.
27. van Bavel, C. H. M., "Measurement of Soil Moisture Content by the Neutron Method USDA-ARD 41–24," U.S. Department of Agriculture, Washington, D.C., 1958.
28. van Bavel, C. H. M., Underwood, N., and Swanson, R. W., "Soil Moisture Measurement by Neutron Moderation," *Soil Science,* Vol. 82, 1956, p. 29.
29. Vasiwani, N. K., "Nuclear Measurement of Subgrade Moisture," *In Situ Measurement of Soil Properties,* ASCE, Vol. 1, June, 1975, pp. 477–496.
30. Vinson, T. S., Bruggers, D. E., and Mahar, L., "Felton-Herron Creek Watershed Infiltration Studies," Final Report for research funded by the Institute of Water Research, Michigan State University, East Lansing, Mich., Sept., 1976.
31. Vinson, T. S., and Davison, B. E., "A Field Study on the Relationship of Temperature and Ice to Infiltration at a Spray Irrigation Facility," *Report No. MSU-CE-75-2,* Institute of Water Research, Michigan State University, East Lansing, Mich., Sept., 1975.

Appendix II.—Notation

The following symbols are used in this paper:

Pr = percolation rate;
k = permeability;
mc = moisture content;
V = velocity;
t = elapsed time from onset of percolation;
dh/dz = hydraulic gradient; and
γ_w = density of water.

DIMENSIONLESS STREAM ADVANCE IN SLOPING BORDERS

By Theodor Strelkoff,[1] M. ASCE and Albert J. Clemmens,[2] A. M. ASCE

INTRODUCTION

A mathematical model (7) of border irrigation has been developed and found both reliable and sufficiently inexpensive in execution to comprise a practical design tool. On the other hand, it does require from a fraction of a minute to several minutes of execution time on a digital computer of intermediate speed and memory capacity (e.g., Burroughs 6700) to simulate the advance, recession, runoff, and ultimate distribution of infiltrated water stemming from given inflow and application time and bed slope, roughness, and infiltration. Furthermore, the results are of course valid only for that one set of input parameters. In common with results of numerical methods in general, the solution obtained gives no clue regarding solution behavior in general. Behavioral trends can be noted only through repeated solution using many different combinations of input variables. Because of the large number of variables governing the outcome of any one irrigation, a comprehensive examination of the effect of each, in dimensional terms, is nearly impossible. Presentation of the results alone would require pages and pages of graphs.

The problem of discerning the general behavior of solutions is greatly simplified by the use of dimensionless notation. Use of such notation reduces the number of independent parameters governing the solution to a tractable value. The result, several pages of dimensionless graphs, displays the overall behavior of the advance function under the most varied input conditions found in practice. Furthermore, through interpolation between curves, the advance for any practical combination of input variables can be obtained directly, without the use of electronic computing equipment.

While the complete mathematical model outlined in (7) has the capability of predicting the entire irrigation, including recession and runoff, the dimensionless solution graphs herein are restricted to the advance phase alone. Recession

[1]Formerly, Prof. of Hydr. Engrg., Univ. of California, Davis, Calif.; Currently, Independent Consultant, 43 Liberty Street, San Francisco, Calif.

[2]Research Hydr. Engr., U.S. Water Conservation Lab., U.S. Dept. of Agr., Sci. and Education Administration, Federal Research, Phoenix, Ariz.

Note.—Discussion open until May 1, 1982. To extend the closing date one month, a written request must be filed with the Manager of Technical and Professional Publications, ASCE. Manuscript was submitted for review for possible publication on December 30, 1980. This paper is part of the Journal of the Irrigation and Drainage Division, Proceedings of the American Society of Civil Engineers, ©ASCE, Vol. 107, No. IR4, December, 1981. ISSN 0044-7978/81/0004-0361/$01.00.

is controlled by more parameters than advance, and representation of the complete theoretical spectrum of recession curves is not yet possible, even with full use of dimensionless notation. This problem is currently under study, and the writers express their optimism, regarding a satisfactory resolution in the future.

An initial study of dimensionless advance was presented in Ref. 3. As pointed out in Ref. 2, the range of variation of the dimensionless variables employed excluded some cases of practical importance. Furthermore, the choice of dimensionless parameters was not optimal and required an excessive number of cycles in presenting the data on logarithmic scales. Finally, the response of the advance function to cutoff of the inflow was ignored. All of these questions are treated in the present paper.

Governing Equations and Boundary Conditions

The governing equations imply conservaton of mass and equilibrium of forces in elements of the surface stream. The forces can be assumed in balance, because accelerations are negligible in border-irrigation flows (3,6). The upstream boundary condition is the discharge hydrograph, typically, an inflow constant, q_0, until cutoff at the end of the application time, t_{co}. The downstream boundary condition during stream advance is zero depth and discharge at the wave front. Initially, depth and discharge are zero everywhere in the border.

The mathematical expressions of these conditions is the following:

$$(\bar{q}_{r_U} - \bar{q}_{r_D})\,\delta t = [(\bar{y} + \bar{z})_t - (\bar{y} + \bar{z})_{t-\delta t}]\,\delta x \quad \ldots\ldots\ldots\ldots\ldots\ldots (1)$$

$$\frac{\gamma y_U^2}{2} - \frac{\gamma y_D^2}{2} + \gamma \bar{y}\,\delta x\, \bar{S}_b - \gamma \bar{d}\,\delta x = 0 \quad \ldots\ldots\ldots\ldots\ldots\ldots\ldots (2)$$

$$\left.\begin{aligned} q_0 &= q_{in} \quad 0 < t \le t_{co} \\ q_0 &= 0 \quad t > t_{co} \end{aligned}\right\} \quad \ldots\ldots\ldots\ldots\ldots\ldots\ldots\ldots (3)$$

$$q = 0 = y \quad x = x_A < L \quad \ldots\ldots\ldots\ldots\ldots\ldots\ldots\ldots (4)$$

$$q = y = 0 \quad t = 0 \quad \ldots\ldots\ldots\ldots\ldots\ldots\ldots\ldots (5)$$

In Eqs. 1-5, q = discharge per unit width; q_r = unit discharge crossing the face of an element of the surface stream; q_{in} = constant unit inflow; y = surface-flow depth; z = subsurface depth (volume infiltrated per unit plan area of border); x = distance down the border; x_A = length of the advancing stream (assumed for this study always less than field length, L); t = time; and t_{co} = cutoff or application time. The subscript, 0, refers to the upstream end of the border; U refers to the upstream face of an element of the surface stream and D the downstream face. The length of the element is δx, while δt is an increment of time. The bar over a variable signifies a time average during δt, the tilde represents a distance average over δx. The bottom slope is given by S_b; γd represents the resistance (drag) of the bed and vegetation per unit plan area of surface stream. It is related to the so-called friction slope, $S_f = d/y$, and is generally a function, $d\,(q, y)$, of depth and discharge at a section, for any given soil-surface and crop geometry. The depth of infiltration at any section, x, is assumed to be a known function of the infiltration time, τ =

$t - t_A(x)$, at that location; $t_A(x)$ is the inverse of the advance function, $x_A(t)$, and represents the time the stream advanced to station x.

General Nondimensionalization of Equations

Equations 1–5 can be put in dimensionless form by first introducing nonzero reference variables Q, T, X, Y, and Z. For the moment, these are undefined, but possess dimensions—length^2/time, time, length, length, and length, respectively. Then dimensionless variables are defined as follows

$$q^* = \frac{q}{Q}; \quad t^* = \frac{t}{T}; \quad t_A^* = \frac{t_A}{T}; \quad y^* = \frac{y}{Y}; \quad x^* = \frac{x}{X}; \quad z^* = \frac{z}{Z};$$

$$t_{co}^* = \frac{t_{co}}{T}; \quad q_{in}^* = \frac{q_{in}}{Q}; \quad L^* = \frac{L}{X} \qquad (6)$$

and are substituted into the governing equations. When Eq. 1 is divided by XY, and Eq. 2 by γY^2, the following dimensionless forms result

$$\Psi^* (\bar{q}_{r_U}^* - \bar{q}_{r_D}^*) \delta t^* = [(\bar{y}^* + K^* \bar{z}^*)_{t^*} - (\bar{y}^* + K^* \bar{z}^*)_{t^* - \delta t^*}] \delta x^* \qquad (7)$$

$$\frac{y_U^{*2}}{2} - \frac{y_D^{*2}}{2} + S_0^* \bar{y}^* s \delta x^* - D^* \bar{d}^* \delta x^* = 0 \qquad (8)$$

$$\left.\begin{aligned} q_0^* &= q_{in}^* \quad 0 < t^* \le t_{co}^* \\ q_0^* &= 0 \quad t^* > t_{co}^* \end{aligned}\right\} \qquad (9)$$

$$q^* = 0 = y^* \quad x^* = x_A^* < L^* \qquad (10)$$

$$q^* = 0 = y^* \quad t^* = 0 \qquad (11)$$

in which $$\Psi^* = \frac{QT}{XY} \qquad (12)$$

$$K^* = \frac{Z}{Y} \qquad (13)$$

$$S_0^* = \frac{S_0}{\frac{Y}{X}} \qquad (14)$$

$$D^* = \frac{\frac{D}{Y}}{\frac{Y}{X}} \qquad (15)$$

The quantity, s = ratio of local bed slope, S_b, to bed slope, S_0, at the head end of the border; in a plane border $s \equiv 1$. The term, d^* = ratio of local drag per unit plan area, d, to drag per unit area, D, computed with reference depth and discharge, $d^* = d(q, y)/D$; and $D = d(Q, Y)$. The infiltration depth is computed as a function of infiltration time, $z = z(t - t_A)$. In order that

dimensionless time t^* and t_A^* appear in Eq. 7 instead of dimensional time, t, and t_A, the reference infiltration depth, Z, must be defined as a function of the characteristic time, $Z = Z(T)$, such that

$$z(t - t_A) = Z(T) \cdot z^*(t^* - t_A^*) \quad \ldots \ldots \ldots \ldots \ldots \ldots \ldots \quad (16)$$

The functional form of Z is usually, but need not be, the same as the functional form of z. The expression of z^* in terms of τ^* depends upon the exact form of the actual and reference infiltration functions; this question is dealt with in a later paragraph.

The solution to Eqs. 7 and 8 in a plane border is controlled by the dimensionless parameters, Ψ^*, K^*, S_0^*, and D^*, by the dimensionless boundary values, q_{in}^*, t_{co}^*, and by the form of the dimensionless infiltration and resistance functions, z^* and d^*.

Selection of Dimensionless Governing Parameters.—Substantial simplification of these equations is achieved by judicious choice of the reference variables Q, T, X, Y, and Z. In previous work in sloping borders (1,3) $Q = q_{in}$, so that $q_{in}^* = 1$, and Y was set to normal depth for the given inflowing discharge, slope, and roughness. This led to the results, $D^* = S_0^*$. The reference infiltration depth was defined in terms of the reference time, $Z = z(T)$, in which z was the given infiltration function. In Ref. 3, T was determined by the condition $Z = Y$, i.e., $K^* = 1$. Then X was found from the additional desired condition $\Psi^* = 1$. Furthermore, in Ref. 3, the two-parameter Kostiakov infiltration formula, $z = k\tau^a$, in which k and a are constants, was used. As a result, the system of Eqs. 7–11, with t_{co}^* and L^* indefinitely large, was governed by only two parameters, a and S_0^*, and dimensionless-advance solutions were presented as a two-parameter family of graphs. Clemmens (2) pointed out that for a given range of the physical variables, k, a, S_0, q_{in}, and Manning n, the same information could be presented over a smaller range of x^*, t^* by requiring instead of $K^* = 1$, the condition $S_0^* = 1$. This defined X; the condition, $\Psi^* = 1$, defined T, and the result was again a two-parameter family of graphs (t_{co}^* and L^* were still considered larger, respectively, than any computed t^* and x^*), with a and K^* the governing parameters.

In Ref. 1, the two-parameter family could have been reduced to one governed by a single parameter, because level borders, with $S_0 = 0$, only, were considered. With $S_0^* = 0$, and Ψ^*, K^*, and D^*, each set to unity to define X, Y, and T, and $Z = kT^a$, the two remaining solution-governing parameters would be a and t_{co}^*; if only $t^* < t_{co}$ were to be considered, as in Ref. 3, a would remain the sole governing parameter. On the other hand, the requirement $K^* = 1$ for all soils, however tight or permeable they may be (e.g., for the entire range of Kostiakov k and a found in practice), leads to enormous variation in T and, thus, X. From this stems the need for many, many cycles of logarithmic paper on which to present graphical advance data. Furthermore, because advance (and recession) after cutoff also was to be considered in Ref. 1, it proved desirable to set $T = t_{co}$. Then, with $\Psi^* = 1$, $D^* = 1$, the resulting two-parameter solution was governed by a and K^*.

The question arises: how may of the dimensionless governing parameters Ψ^*, K^*, S_0^*, D^* q_{in}^*, t_{co}^*, etc., can be controlled independently of the physical parameters of the irrigation? A corollary question is—what is the minimum number of parameters governing the solution of Eqs. 7–11?

Eqs. 12–15 and the last two parts of Eq. 6 can be rewritten as equations defining the interrelationship between the reference variables and the dimensionless governing parameters in terms of the physical parameters of the irrigation

$$\frac{XY\Psi^*}{QT} = 1 \quad \ldots \quad (17)$$

$$\frac{K^* Y}{Z(T)} = 1 \quad \ldots \quad (18)$$

$$\frac{YS_0^*}{X} = S_0 \quad \ldots \quad (19)$$

$$\frac{Y^2 D^*}{Xd(Q, Y)} = 1 \quad \ldots \quad (20)$$

$$Q\, q_{\text{in}}^* = q_{\text{in}} \quad \ldots \quad (21)$$

$$T\, t_{\text{co}}^* = t_{\text{co}} \quad \ldots \quad (22)$$

The six equations, Eqs. 17–22, must be satisfied, whatever are the values ultimately taken on by the six dimensionless parameters, Ψ^*, K^*, S_0^*, D^*, q_{in}^*, t_{co}^*, and the four reference variables, Q, T, Y, and X; no other criteria need be met. Thus, there is considerable leeway in assigning values to these quantities. Comparison of the number of variables to be given values, namely 10, with the number of equations relating these values, six, suggests that four variables can be chosen arbitrarily, with the remaining six stemming from solution of the six equations. On the other hand, the particular structure of these equations introduces constraints and reduces the degree of freedom that can be exercised in choosing those variables to be assigned arbitrary values. For example, Eq. 19, alone, shows that even the three quantities, Y, X, and S_0^* cannot be given arbitrary values.

Thus, as mentioned previously, in Ref. 3 Y was set to normal depth for q_{in} and S_0, and Ψ^*, q_{in}^*, and K^* were each set to unity. This left S_0^* $(= D^*)$ and t_{co}^* to govern the dimensionless solution together with whatever parameters were introduced by the infiltration and friction-slope functions. In Ref. 3, t_{co}^* was assumed larger than the largest t^* considered, so that in the last analysis, it (like L^*) played no role.

In Ref. 2, Y was again set to normal, so $S_0^* = D^*$, and Ψ^*, q_{in}^*, and S_0^* were set to unity. The dimensionless solution was then governed by K^* and t_{co}^* and by parameters from the infiltration and friction functions. Again, t_{co}^* was set in excess of all t^* to reduce the total number of governing parameters.

In Ref. 1, $S_0 = 0$; therefore, from Eq. 19, $S_0^* = 0$. Of the seven unknowns, X, Y, Ψ^*, q_{in}^*, t_{co}^*, D^*, and K^*, the four, Ψ^*, q_{in}^*, t_{co}^*, and D^* were all set to unity, and Eqs. 17 and 20 yielded X and Y. Equation 18 gave K^*, which along with the parameters of the infiltration and friction functions, governed the dimensionless solution.

Infiltration Functions.—In Refs. 1, 2, and 3, the infiltration function adopted was the Kostiakov formula

$$z(\tau) = k\tau^a \quad \ldots \quad (23)$$

The same functional form was used for Z. This led to a simple result for

$$z^*(\tau^*), \quad \text{namely} \quad z^*(\tau^*) = \tau^{*a} \quad \ldots\ldots\ldots\ldots\ldots\ldots\ldots\ldots \quad (24)$$

Thus, in addition to whatever other dimensionless parameters governed the solution, the parameter, a, stemming from the infiltration function also played a role.

If the variable representing irrigation times becomes quite large, the Kostiakov formula gives too small an infiltration rate, and fails to reproduce the constant rate exhibited by many soils at large infiltration times. The following modification of the Kostiakov equation

$$z(\tau) = k\tau^a + b\tau \quad \ldots\ldots\ldots\ldots\ldots\ldots\ldots\ldots\ldots\ldots\ldots\ldots \quad (25)$$

allows a nonzero final infiltration rate, but now an additional governing parameter arises, as can be seen from the corresponding dimensionless infiltration function

$$z^*(\tau^*) = \frac{1}{1+b^*}\tau^{*a} + \frac{b^*}{1+b^*}\tau^* \quad \ldots\ldots\ldots\ldots\ldots\ldots\ldots\ldots \quad (26)$$

To obtain Eq. 26, the functional forms of Z and z were again made identical, i.e., $Z = z(T)$. The two parameters stemming from the infiltration formula are now a and b^*, the latter given by

$$b^* = \frac{bT}{kT^a} \quad \ldots\ldots\ldots\ldots\ldots\ldots\ldots\ldots\ldots\ldots\ldots\ldots \quad (27)$$

The Philip formula (5), $z = S\tau^{1/2} + A\tau$, is a special case of Eq. 25, and leads to but one infiltration-based free parameter, given by

$$b^* = \frac{AT}{ST^{1/2}} \quad \ldots\ldots\ldots\ldots\ldots\ldots\ldots\ldots\ldots\ldots\ldots\ldots \quad (28)$$

It is possible to develop a more direct approach than Eq. 25 for synthesizing an infiltration function which reflects both the high initial rate characteristic of the Kostiakov formula and a constant final infiltration rate i_f. A two-branch function is suggested, the branches meeting at the time, τ_f, when the rate given by the Kostiakov formula equals i_f. Then

$$\left.\begin{aligned} z &= k\tau^a \quad \tau \le \tau_f \\ z &= k\tau_f^a + i_f(\tau - \tau_f) \quad \tau \ge \tau_f \end{aligned}\right\} \quad \ldots\ldots\ldots\ldots\ldots\ldots\ldots\ldots \quad (29)$$

$$\text{Note that} \quad \tau_f = \left(\frac{i_f}{ak}\right)^{1/(a-1)} \quad \ldots\ldots\ldots\ldots\ldots\ldots\ldots\ldots \quad (30)$$

Such a function is more easily obtained from a plot on logarithmic paper of measured infiltration rate against time than the function of Eq. 25. If Z were again chosen as equal to $z(T)$, dimensionless infiltration, z^*, as a function of dimensionless infiltration time, τ^*, would have four branches depending upon whether $\tau < \tau_f$, or $\tau > \tau_f$ and upon whether $T < \tau_f$, or $T > \tau_f$. The dimensionless function can be described with but two branches, as follows, if the reference infiltration function is set to $Z = kT^a$. Then

$$\left.\begin{aligned} z^* &= \tau^{*a} \quad \tau^* < \tau_f^* \\ z^* &= \tau_f^{*a}(1-a) + i_f^* \tau^* \quad \tau^* > \tau_f^* \end{aligned}\right\} \quad \ldots\ldots\ldots\ldots\ldots\ldots\ldots\ldots \quad (31)$$

$$\text{in which} \quad \tau_f^* = \left(\frac{i_f^*}{a}\right)^{1/(a-1)} \quad \ldots\ldots\ldots\ldots\ldots\ldots\ldots\ldots \quad (32)$$

$$\text{and} \quad i_f^* = \frac{i_f T}{k T^a} \quad \ldots\ldots\ldots\ldots\ldots\ldots\ldots\ldots \quad (33)$$

The two-branch function, Eq. 31, then, introduces two additional dimensionless parameters, a and i_f^*, into the set governing solution of Eqs. 7–11.

Resistance Functions.—Next, solution-governing parameters stemming from the choice of resistance function are considered. With the Manning formula, the drag per unit area is given by

$$d = \frac{q^2}{\left(\frac{C_u}{n}\right)^2 y^{7/3}} \quad \ldots\ldots\ldots\ldots\ldots\ldots\ldots\ldots \quad (34)$$

in which C_u is a units coefficient ($C_u = 1.0\ \mathrm{m}^{1/2}/\mathrm{s}$ in the Standard International, SI, system of units; $C_u = 1.4859\ \ldots\ \mathrm{ft}^{1/2}/\mathrm{sec}$ in the English system), and n is the Manning roughness coefficient. Now, the reference drag per unit area is

$$D = \frac{Q^2}{\left(\frac{C_u}{n}\right)^2 Y^{7/3}} \quad \ldots\ldots\ldots\ldots\ldots\ldots\ldots\ldots \quad (35)$$

$$\text{and} \quad d^* = \frac{q^{*2}}{y^{*7/3}} \quad \ldots\ldots\ldots\ldots\ldots\ldots\ldots\ldots \quad (36)$$

Thus, no additional parameters are introduced into Eqs. 7–11.

With the Sayre-Albertson formula (4), the drag per unit area is

$$d = \frac{q^2}{36.7\, g \left(\log \frac{y}{\chi}\right)^2 y^2} \quad \ldots\ldots\ldots\ldots\ldots\ldots\ldots\ldots \quad (37)$$

in which g = ratio of unit weight to mass density $g = 32.2\ \mathrm{ft/sec^2}$ in English units, ($g = 9.81\ \mathrm{m/s^2}$ in SI units), and χ = an absolute-roughness measure investigated in irrigation borders by Kruse (4). With $D = d(Q, Y)$, the relative drag per unit area is given by

$$d^* = \frac{q^{*2}}{y^{*2}\left(\frac{\log y^*}{\log \chi^*} - 1\right)^2} \quad \ldots\ldots\ldots\ldots\ldots\ldots\ldots\ldots \quad (38)$$

Evidently, this form of the resistance formula introduces an additional solution-governing dimensionless parameter χ^*, defined

$$\chi^* = \frac{\chi}{Y} \quad \ldots \ldots \ldots

less-solution parameters for advance smaller than field length and for advance times smaller than application time, is one, plus those stemming from the particular choice of infiltration and resistance formulas. With the Kostiakov and Manning

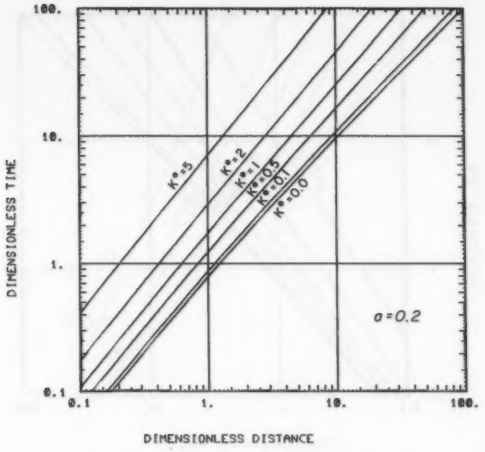

FIG. 3.—Dimensionless Advance; $a = 0.2$

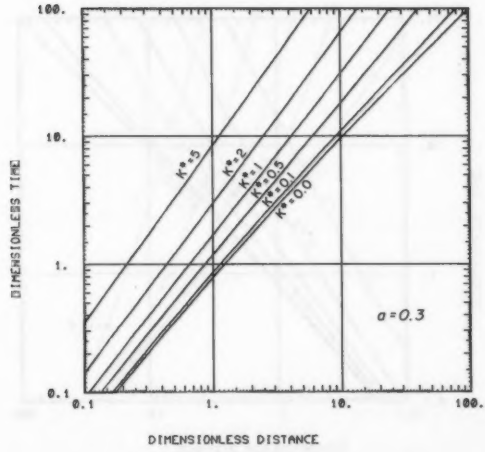

FIG. 4.—Dimensionless Advance; $a = 0.3$

equations, one additional parameter, a, is introduced. A Kostiakov formulation modified to yield a constant final infiltration rate as per Eqs. 25 or 29 requires

one additional free parameter while the Sayre-Albertson resistance formula introduces one more. Introduction of cutoff time as a pertinent variable leads to an additional dimensionless solution parameter.

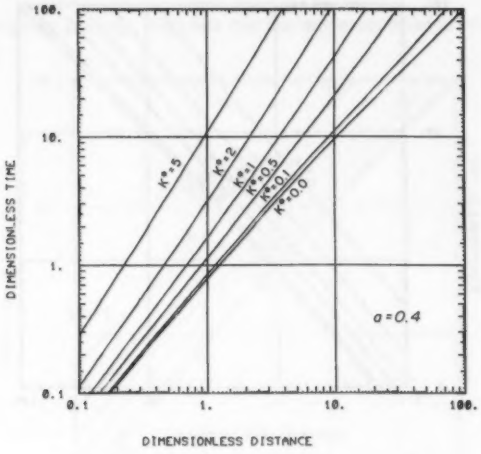

FIG. 5.—Dimensionless Advance; $a = 0.4$

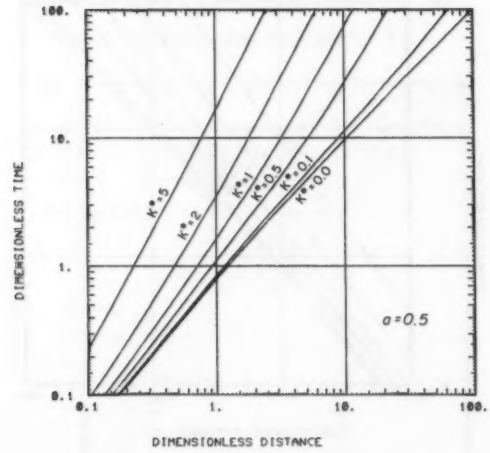

FIG. 6.—Dimensionless Advance; $a = 0.5$

Generalized advance curves are presented for sloping borders of indefinite length with resistance expressible in terms of the Manning n and infiltration

characteristics defined by the Kostiakov power law. Because finite application times are considered, the minimum number of solution parameters is three.

In principle, a one-parameter family of dimensionless advance curves can

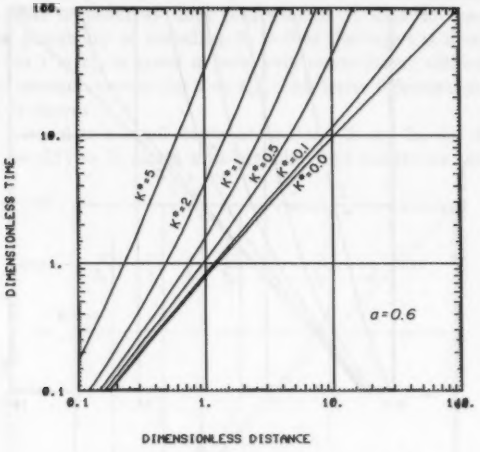

FIG. 7.—Dimensionless Advance; $a = 0.6$

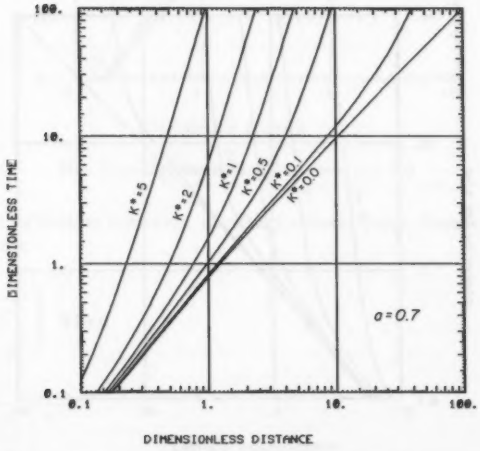

FIG. 8.—Dimensionless Advance; $a = 0.7$

be shown on one sheet of graph paper; each curve, x^* versus t^*, would correspond to a different value of the parameter. A two-parameter family requires a booklet

of pages (as in Refs. 1 and 3), each page corresponding to a different value of the second parameter. A three-parameter family requires then, in general, a series of booklets, each identified by the value of the third parameter.

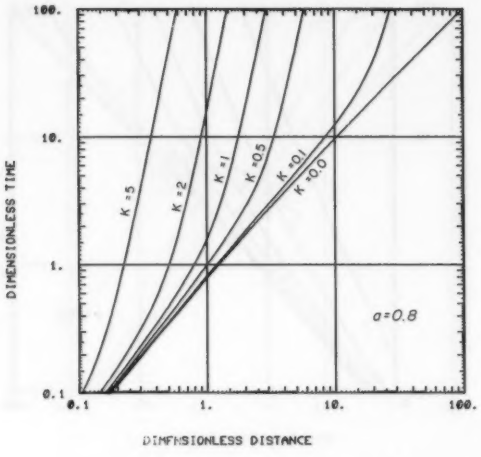

FIG. 9.—Dimensionless Advance; $a = 0.8$

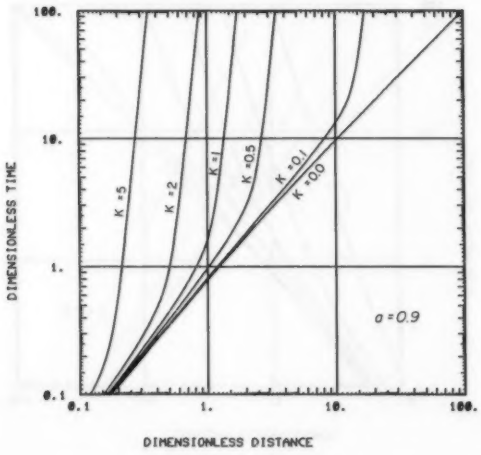

FIG. 10.—Dimensionless Advance; $a = 0.9$

Such would have been the requirement for presenting generalized advance data, including advance after cutoff, if the otherwise desirable choice was made

in Eqs. 17–22, $V^* = 1$; $D^* = 1$; $q^*_{in} = 1$; and $t^*_{co} = 1$. Then the parameters $0 \le K^* \le K^*_{max}$; $0 < a < 1$; $0 \le S^*_0 \le S^*_{0_{max}}$ (with K^*_{max} and $S^*_{0_{max}}$ representing reasonable upper limits) would cover all possible physical variation in (Kostiakov) infiltration and bed slope, including impervious soil and horizontal borders as special cases. But in order to limit presentation of data to essentially one "booklet," the possibility of including $S_0 = 0$ in the series is disallowed, and advance data for $t > t_{co}$ is given in relatively crude form, without the detail evident in the advance curves for $t \le t_{co}$. The latter information is given in a separate set of curves.

By setting Y equal to normal depth as in Refs. 2 and 3, and $V^* = 1$; $q^*_{in} = 1$; and D^* $(= S^*_0) = 1$; along with Manning and Kostiakov the respective

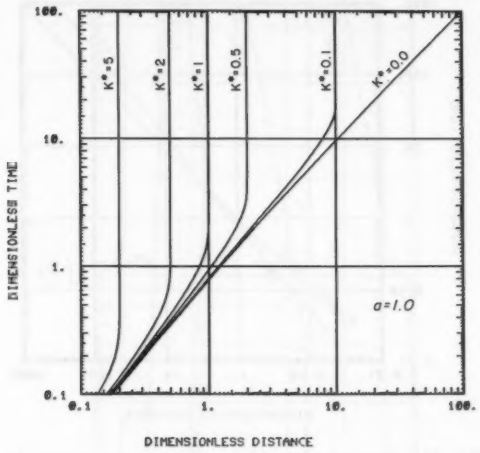

FIG. 11.—Dimensionless Advance; $a = 1.0$

resistance and infiltration functions, the characteristic depth, distance, and time, respectively, are

$$Y = \left(\frac{q_{in}}{\sqrt{S_0}\,\dfrac{C_u}{n}} \right)^{3/5} \qquad (40)$$

$$X = \frac{q_{in}^{3/5}}{S_0^{13/10}\left(\dfrac{C_u}{n}\right)^{3/5}} \qquad (41)$$

$$T = \frac{q_{in}^{1/5}}{S_0^{8/5}\left(\dfrac{C_u}{n}\right)^{6/5}} \qquad (42)$$

The dimensionless solution-governing parameters are then a, K^*, and t^*_{co}. The graphs are organized around these three parameters as follows. Dimensionless advance, x^*_A, prior to cutoff is presented as a function of dimensionless time, t^*, with dimensionless infiltration, K^*, and exponent, a, as parameters. This effectively eliminates, for the present, t^*_{co} as a governing parameter because, physically, advance is not affected by t_{co}, prior to $t = t_{co}$. A page of graphs is presented for each value of $0 \leq a \leq 1$ in increments of 0.1 (Figs. 1–11). The solution curves were obtained by means of the numerical methods described in Ref. 7.

The range of dimensionless variables presented stems from the extensive survey of dimensional irrigation parameters encountered in practice described

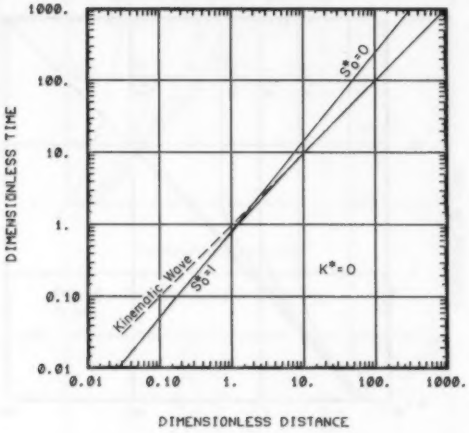

FIG. 12.—Dimensionless Advance over an Impervious Bed

in Ref. 2. The ranges adopted are

$$2 < q_{in} < 25 \quad \text{L/sm} \quad \ldots \quad (43)$$

$$0.5 < t_{co} < 5 \text{ hr} \quad \ldots \quad (44)$$

$$0.0001 < S_o < 0.01 \quad \ldots \quad (45)$$

$$0.02 < n < 0.25 \quad \ldots \quad (46)$$

$$1 < k < 12 \quad \text{cm/hr}^a \quad \ldots \quad (47)$$

$$0 < a < 1 \quad \ldots \quad (48)$$

$$100 < L < 500 \text{ m} \quad \ldots \quad (49)$$

These lead, with the aforementioned system for nondimensionalization, to the following ranges of dimensionless time and distance

$$.01 < x^*_A < 500 \quad \ldots \quad (50)$$

$$0.1 < t^* < 4000 \quad \ldots \quad (51)$$

and dimensionless infiltration

$.01 < K^* < 13$ for $a = 0.0$

$.01 < K^* < 5$ for $a = 0.5$

$.01 < K^* < 25$ for $a = 1.0$ . . . . . (52)

Considering: (1) The values of x_A^* and K^* resulting from input-variable combinations actually found in the field (as opposed to artificial combinations

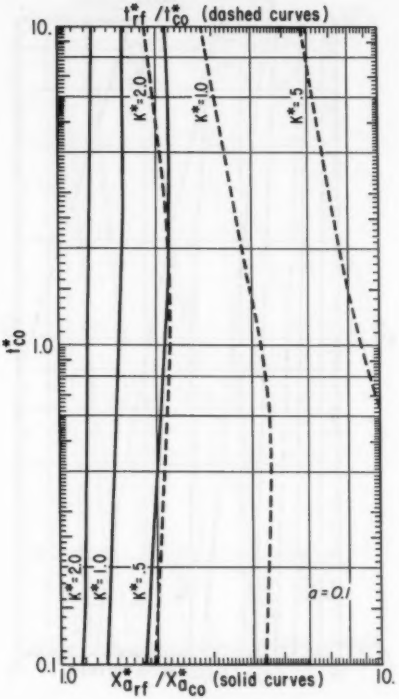

FIG. 13.—Maximum Advance (Incipient Front-End Recession) after Cutoff; Distance and Time; $a = 0.1$

of extremes taken from different sets of field data); and (2) the aforementioned limits of x_A^*, t^*, and K^* found from such artificial combinations, the following limits are expected to cover the range of conditions pertinent to sloping borders:

$0.1 < x_A^* < 100$ . . . . . (53)

$0.1 < t^* < 100$ . . . . . (54)

$$0 < K^* < 5 \quad \ldots\ldots\ldots\

to Eqs. 7, 9–11, and 56 is then the same as one obtained from Eqs. 7–11 with $S_0^* = 0$. This solution is shown in Fig. 12, and is indeed seen to be the limit of the general solution when t^* is very small. As proven in Ref. 1, this curve has the constant slope 16/13 when plotted on logarithmic paper. At the other extreme, when t^* is very large, the advance rate becomes uniform as the profile assumes its ultimate shape. Then, the slope of the advance curve on logarithmic paper is simply unity, thus, explaining the observed curvature

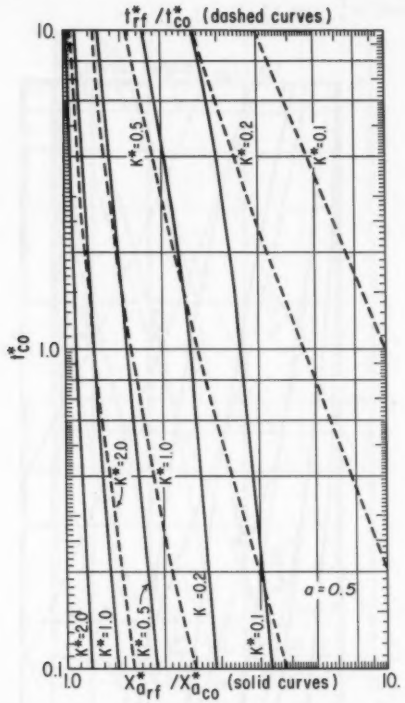

FIG. 15.—Maximum Advance (Incipient Front-End Recession) after Cutoff; Distance and Time; $a = 0.5$

of the general advance curve with $K^* = 0$. Further, with the particular system of nondimensionalization employed, the dimensionless speed of advance is also unity. Indeed, under ultimate conditions, with a fixed profile shape moving down the border, advance rate equals the velocity of flow at the upstream end of the border. There, $q_0^* = 1$; and $y_0^* = 1$; thus, $dx_A^*/dt^* = q_0^*/y_0^* = 1$.

Advance After Cutoff.—Once the irrigation stream has been cutoff, the advance slows. With a sloping impervious bed, $K^* = 0$, advance continues indefinitely though at an ever-decreasing rate. With infiltration, however, the advancing

stream eventually halts and then recedes back up the border. The curve of advance after cutoff approaches some maximum advance distance, $x^*_{A_{max}}$, at a time, $t^*_{A_{max}}$, which represents the termination of advance and the beginning of front-end recession. The maximum advance distance and associated time are shown in Figs. 13–17 for $a = 0.1$–0.9 in steps of 0.2. Both time (dashed lines) and distance (solid lines) are shown relative to the values of each at cutoff. For high values of K^*, front-end recession occurs almost immediately after cutoff ($t^*_{A_{max}} \rightarrow t^*_{co}$) and the stream advances only a short distance beyond its location at cutoff ($x^*_{A_{max}} \rightarrow x^*_{A_{co}}$).

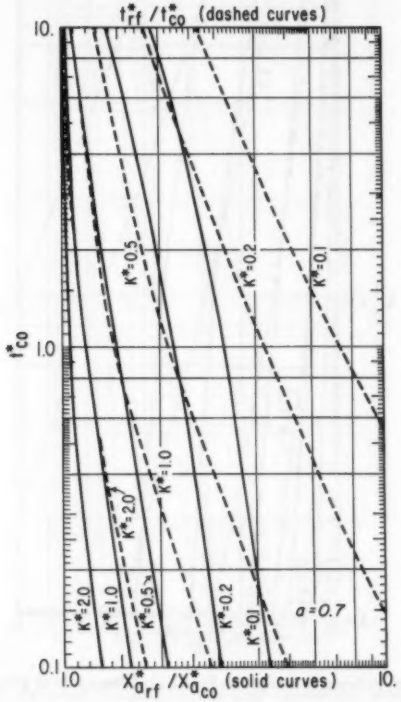

FIG. 16.—Maximum Advance (Incipient Front-End Recession) after Cutoff; Distance and Time; $a = 0.7$

It is usually undesirable for the field length to be greater than the maximum advance distance since part of the border would receive no water at all. But knowledge of the maximum advance distance and its associated time can be used to construct an approximate curve of advance after cutoff, even if the theoretical maximum advance is greater than field length. After calculating the appropriate values of T, X, K^*, and t^*_{co} and L^*, Figs. 1–11 are used with

the appropriate a value to construct the curve for advance prior to cutoff. Then Figs. 13–17 are used to determine the maximum advance distance and its associated time. The curve for advance after cutoff can then be sketched in through the two known points $[(x_{A_{co}}, t_{co})$ and $(X_{A_{max}}, t_{A_{max}})]$ with the requirement that it be tangent to the curve for advance prior to cutoff at the time of cutoff and tangent to the vertical (x = const) at the end of advance. At any event, the advance curve so constructed beyond $x = L$ is simply ignored.

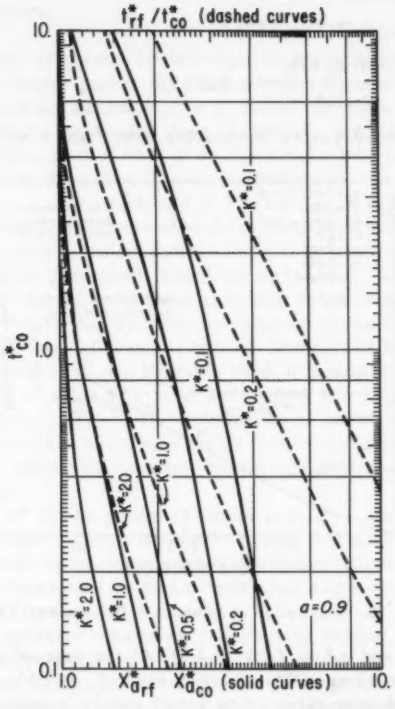

FIG. 17.—Maximum Advance (Incipient Front-End Recession) after Cutoff; Distance and Time; a = 0.9

Example

Determine the advance curve for the following situation: L = 1200 ft (366 m); q = 0.08 ft^2/sec (7.432 L/sm); n = 0.15; S_0 = 0.001; a = 0.7; k = 2.0 in./hr^a (5.08 cm/hr^a); t_{co} = 80 min.

From Eq. 40 (with units in meters and seconds)

$$Y = \left[\frac{q_{in}(n/C_u)}{\sqrt{S_0}}\right]^{3/5} = \left[\frac{0.007432 \cdot 0.15}{\sqrt{0.001}}\right]^{3/5}$$

From Eq. 19 (since $S_0^* = 1$)

$$X = \frac{Y}{S_0} = \frac{0.1344}{0.001} = 134.4 \text{ m}$$

From Eq. 17 (since $V^* = 1$; $Q = q_{in}$)

$$T = \frac{XY}{q_{in}} = \frac{134.4 \cdot 0.1344}{0.007432} = 2430 \text{ sec} = 40.5 \text{ min} = 0.675 \text{ hr}$$

From Eq. 18 (since $Z(T) = kT^a$)

$$K^* = \frac{kT^a}{Y} = \frac{(0.0508) \cdot (0.675)^{0.7}}{0.1344} = 0.287$$

The advance curve can be constructed from Figs. 8 and 16 in which t_{co}^*

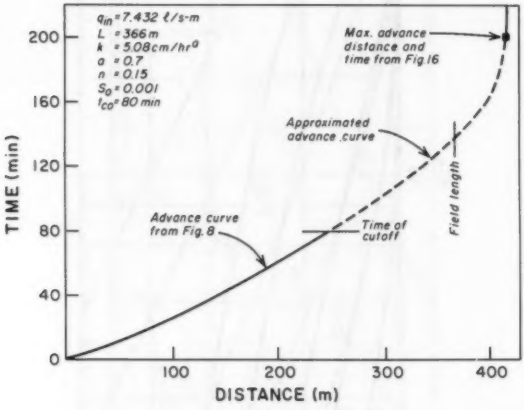

FIG. 18.—Illustration of Advance in Dimensional Terms

$= t_{co}/T = 1.98$ and $L^* = L/X = 2.72$. At the time of cutoff ($t^* = t_{co}^*$) for $K^* \cong 0.3$, the advance distance (Fig. 8) is $x_{a_{co}}^* \cong 1.85$; or $x_{A_{co}} = x_{a_{co}}^* \cdot X = 250$ m. The advance curve up to cutoff can be constructed by choosing lower values of t^* and the corresponding x_A^*. The maximum possible advance distance (Fig. 16) is $x_{a_{rf}}^*/x_{a_{co}}^* \cong 1.65$ or $x_{a_{rf}} \cong 1.6 \cdot 250$ m $= 412$ m. The corresponding time is $t_{rf}^*/t_{co}^* \cong 2.5$ or $t_{rf} = 2.5 \cdot 80$ min $= 200$ min. The entire advance curve can now be constructed as in Fig. 18; the curve after cutoff is tangent to advance at cutoff and to the vertical at the maximum advance distance. The total advance time for the given field length from Fig. 18 is roughly 136 or 137 min, which is very close to the time computed with the computer model directly, namely 136.1 min. From the computer solution of this example (which includes recession), the application efficiency (net application/gross application) for a 3 in. (7.62 cm) net application was 78% with 7% runoff.

It is important to note that interpolation between curves can be subject to error. However, errors in estimating maximum advance distances and times will produce minor errors unless the field length is very close to maximum advance distance. The major source of error will normally be in determining advance prior to cutoff. If interpolation is questionable, plot advance distances at any given time, t^*, for the K^* values presented, and graphically determine the advance distance for the desired K^* value.

Summary and Conclusions

The simplest case of general border-irrigation advance is characterized by a plane border of length greater than any advance distance of interest, and by a constant inflowing discharge prior to cutoff. In this case, the advance curve is controlled by the border slope, roughness, and infiltration, and by the inflow discharge and cutoff time. If the Manning formula is used to describe the roughness and the Kostiakov formula the infiltration, the advance function is controlled by q_{in}, t_{co}, S_0, n, k, and a. The number of controlling variables is significantly reduced—to three—when the problem is viewed in dimensionless terms. If advance prior to inflow cutoff only is of interest, two dimensionless parameters govern the dimensionless advance curves.

If a and S_0^* are chosen to be those governing parameters (by setting Y = normal depth, $K^* = 1$), an extraordinary range of variation of x^* and t^* is needed to cover all cases of practical interest. The case of an impervious bed cannot be represented at all. On the other hand, it is possible to show directly from the curves of x^* (t^*, a, S_0^*), as in Ref. 3, how kinematicwave conditions are approached at large $S_0^* x^*$. This information is useful in establishing the range of application of kinematic-wave theory to computation of border-irrigation flow, a procedure simpler than the zero-inertia (equilibrium) analysis employed for the general case.

Use of a and K^* as the governing parameters (Y = normal depth; $S_0^* = 1$) disallows so simple a comparison between zero-inertia and kinematic-wave solutions, but permits the whole spectrum of dimensional parameters encountered in practice to be represented by data covering just a few cycles of logarithmic paper.

With t_{co} as a pertinent controlling variable, the number of dimensionless governing parameters increases to three. If the cutoff time were made the characteristic time, dimensionless solution would be governed by a, S_0^*, and K^*. This would have the advantage of allowing representation of all slopes, including zero slope, and all infiltration rates, including zero, in the one set of curves. This entails, however, a major disadvantage, the difficulty of representing a three-parameter family of advance curves x^* (t^*, a, S_0^*, K^*).

In this work, a compromise was achieved by using normal depth as the characteristic depth and setting $S_0^* = 1$. This no longer permits consideration of horizontal borders, but these were extensively studied in Ref. 1. Prior to cutoff, the advance curves are controlled by a and K^*, and this two-parameter family is presented in Figs. 1–11. Advance after cutoff is viewed approximately in Figs. 13–20, which give the end points of this portion of the advance curve and some indication of how the curve may be sketched in between the starting point, at $(x_{A_{co}}, t_{co})$ and the end point, at $(x_{A_{max}}, t_{A_{max}})$.

Taken together, these curves represent all practical cases of advance of an irrigation stream over a plane border with inflow that is constant prior to cutoff.

Acknowledgments

The writers are grateful for the support given this project by the Science and Education Administration, U.S. Department of Agriculture, under Cooperative Agreement 3092-H.

Appendix.—References

1. Clemmens, A. J., and Strelkoff, T., "Dimensionless Advance for Level-Basin Irrigation," *Journal of the Irrigation and Drainage Division*, ASCE, Vol. 105, No. IR3, Proc. Paper 14820, Sept., 1979, pp. 259–273.
2. Katapodes, N. D., and Strelkoff, T., "Dimensionless Solutions of Border-Irrigation Advance," discussion by Clemmens, A. J., *Journal of the Irrigation and Drainage Division*, ASCE, Vol. 104, No. IR3, Proc. Paper 13980, Sept., 1978, pp. 339–341.
3. Katopodes, N. D., and Strelkoff, T., "Dimensionless Solutions of Border-Irrigation Advance," *Journal of the Irrigation and Drainage Division*, ASCE, Vol. 103, No. IR4, Proc. Paper 13400, Dec., 1977, pp. 401–417.
4. Kruse, E. G., "Flow Resistance in Simulated Irrigation Borders and Furrows," *Conservation Research Report No. 3*, Agricultural Research Service, U.S. Department of Agriculture, U.S. Government Printing Office, Nov., 1965.
5. Philip, J. R., "The Theory of Infiltration: 4. Sorptivity and Algebraic Infiltration Equations," *Soil Science*, Vol. 84, pp. 257–264, 1957.
6. Strelkoff, T., and Katopodes, N. D., "Border-Irrigation Hydraulics with Zero Inertia," *Journal of the Irrigation and Drainage Division*, ASCE, Vol. 103, No. IR3, Proc. Paper 13189, Sept., 1977, pp. 325–342.

TECHNICAL NOTES

Note.—Discussion open until May 1, 1982. To extend the closing date one month, a written request must be filed with the Manager of Technical and Professional Publications, ASCE. This paper is part of the Journal of the Irrigation and Drainage Division, Proceedings of the American Society of Civil Engineers, ©ASCE, Vol. 107, No. IR4, December, 1981.

Technical Notes

To provide a place within ASCE for publication of technical ideas that have not advanced, as yet, to the point where they warrant publication as a Proceedings paper in a *Journal,* the publication of Technical Notes was authorized by the Board of Direction on October 16–18, 1967, under the following guidelines:

1. An original manuscript and two copies are to be submitted to the Manager of Technical and Professional Publications, ASCE, 345 East 47th Street, New York, N.Y., 10017, along with a request by the author that it be considered as a Technical Note.
2. The two copies will be sent to an appropriate Technical Division or Council for review.
3. If the Division or Council approves the contribution for publication, it shall be returned to Society Headquarters with appropriate comments.
4. The technical publications staff will prepare the material for use in the earliest possible issue of the *Journal,* after proper coordination with the author.
5. Each Technical Note is not to exceed 4 pages in the *Journal.* As an approximation, each full manuscript page of text, tables, or figures is the equivalent of one-half a *Journal* page.
6. The Technical Notes will be grouped in a special section of each *Journal.*
7. Information retrieval abstracts and key words will be unnecessary for Technical Notes.
8. The final date on which a Discussion should reach the Society is given as a footnote with each Technical Note.
9. Technical Notes will not be included in *Transactions.*
10. Technical Notes will be included in ASCE's annual and cumulative subject and author indexes.

The manuscripts for Technical Notes must meet the following requirements:

1. Titles must have a length not exceeding 50 characters and spaces.
2. The author's full name, Society membership grade, and a footnote reference stating present employment must appear on the first page of the manuscript. Authors need not be Society members.
3. The manuscript is to be submitted as an original copy (with two duplicates) that is typed double-spaced on one side of 8-1/2-in. (220-mm) by 11-in. (280-mm) white bond paper.
4. All mathematics must be typewritten and special symbols must be properly identified. The letter symbols used must be defined where they first appear, in figures or text, and arranged alphabetically in an Appendix.—Notation.
5. Standard definitions and symbols must be used. Reference must be made to the lists published by the American National Standards Institute and to the *Authors' Guide to the Publications of ASCE.*
6. Tables must be typed double-spaced (an original ribbon copy and two duplicate copies) on one side of 8-1/2-in. (220-mm) by 11-in. (280-mm) paper. An explanation of each table must appear in the text.
7. Figures must be drawn in black ink on one side of 8-1/2-in. (220-mm) by 11-in. (280-mm) paper. Because figures will be reproduced with a width of between 3 in. (76 mm) to 4-1/2 in. (110 mm), the lettering must be large enough to be legible at this width. Photographs must be submitted as glossy prints. Explanations and descriptions must be made within the text for each figure.
8. References cited in text must be typed at the end of the Technical Note in alphabetical order in an Appendix.—References.
9. Dual units, i.e., U.S. Customary followed by SI (International System) units in parentheses, should be used throughout the paper.

Relative Runoff by Curve Number Nomograph

By Richard J. Heggen,[1] A. M. ASCE

Introduction

In many drainage analyses, the Soil Conservation Service (SCS) curve number (CN) runoff volume estimate may serve as initial basis for design of engineering structures (6,7). While there are often a variety of runoff-estimation techniques available having a sounder basis in theory than the CN procedure, these methods are more often appropriate for subsequent, data-intensive studies (2,9).

The CN method weighs runoff-influencing effects of watershed condition and has been pragmatically incorporated into a variety of engineering procedures (1,3,4,5,8). The SCS has cataloged soils by hydrologic families and reported the variation of CN with antecedent moisture, land condition and use, vegetative type and cover, and soil type. SCS soil survey studies often comprise the majority of compiled data available for preliminary hydrologic evaluations (7,10). Whereas other methods may more accurately predict runoff hydrograph peaks and times of concentration, the CN method can rapidly and efficiently appraise the volumetric sensitivity of the hydrograph to changes in watershed condition.

Relative increase in runoff is a paramount technical issue in urbanizing areas where land use changes are only allowed if increased runoff can be retained. It is suggested that while more theoretical or statistical methods should generally be used to estimate the time-dependent magnitude of discharge, CN analysis may be used to explore the relative dependency of this magnitude on watershed condition.

Relative Runoff

Discharge volume may be estimated by the SCS dimensionless standard formulation (6)

$$Q = \frac{(P - 0.2S)^2}{P + 0.8S}; \quad P > 0.2S \quad \ldots\ldots\ldots\ldots\ldots\ldots\ldots\ldots\ldots\ldots (1)$$

in which Q = runoff in inches (cm); P = precipitation in inches (cm); and

[1]Asst. Prof., Dept. of Civ. Engrg., The Univ. of New Mexico, Albuquerque, N.M. 97131.

Note.—Discussion open until May 1, 1982. To extend the closing date one month, a written request must be filed with the Manager of Technical and Professional Publications, ASCE. Manuscript was submitted for review for possible publication on December 31, 1980. This paper is part of the Journal of the Irrigation and Drainage Division, Proceedings of the American Society of Civil Engineers, ©ASCE, Vol. 107, No. IR4, December, 1981. ISSN 0044-7978/81/0004-0385/$01.00.

S = potential maximum retention in inches (cm). In the inch system, the parameter, S, is estimated

$$S = \frac{1000}{CN} - 10 \quad \ldots \ldots \ldots

$$\frac{Q_2}{Q_1} = \left(\frac{P - \dfrac{200}{CN_2} + 2}{P - \dfrac{200}{CN_1} + 2} \right)^2 \left(\frac{P + \dfrac{800}{CN_1} - 8}{P + \dfrac{800}{CN_2} - 8} \right) \quad \ldots\ldots\ldots\ldots\ldots\ldots\ldots (4)$$

in which Q_2/Q_1 represents relative runoff.

It should be noted that unlike relative discharge estimates by the rational formula, this ratio depends on precipitation also. Abstractions from a light rainfall influence runoff to a larger degree than do abstractions from a heavy rainfall.

Eq. 4 may be graphically solved by Fig. 1. Vertical and horizontal nomographs are used to intersect the left-hand and upper sides, respectively, of the rectangular chart. The curve corresponding to the Cartesian coordinate defined by these two intersections indicates relative runoff. A brief example shows the procedure. Let $CN_1 = 77$; $CN_2 = 84$; and $P = 3.5$ in. (9.89 cm). Using 77 and 3.5 to enter the chart from the top and 77 and 84 to enter from the left, a relative discharge of 1.36 is interpolated between the curves. The change in CN increases discharge 36%. If $P = 6$ in. (15.24 cm), the relative change due to curve number would be 20%.

Two limiting lines can be identified on Fig. 1. The first, a vertical line running upward from the point of coincidence on the right, represents a relative discharge of infinity. The second, a 45° line running downward and to the left from the same point of coincidence represents a relative discharge of zero. Points on and to the right of this line violate the constraint given with Eq. 1.

Summary and Conclusion

The graphical solution for relative discharge provides a rapid means for estimating runoff changes due to watershed modification. The graphical solution allows visual appraisal of the sensitivity of runoff change to both CN modification and storm precipitation. Eq. 4 may be used for more accurate calculation, but it should be noted that any analysis based on curve numbers is at best an approximate solution. For problems where actual discharge can be measured or estimated by alternative methods, graphical estimation of relative change provides a pragmatic basis for anticipating runoff modification.

Appendix I.—References

1. Aron, G., Miller, A. C., Jr., and Lakatos, D. F., "Infiltration Formula Based on SCS Curve Number," *Journal of the Irrigation and Drainage Division*, ASCE, Vol. 103, No. IR4, Proc. Paper 13427, Dec., 1977, pp. 419–427.
2. "Flood Flow Frequency for Ungaged Watersheds: A Literature Review," ARS-NE-86, USDA, ARS, Beltsville, Md., Nov., 1977, 136 pp.
3. Hawkins, R. H., "The Importance of Accurate Curve Numbers in the Estimation of Storm Runoff," *Water Resources Bulletin*, Vol. 11, No. 5, Oct., 1975, pp. 887–891.
4. Hawkins, R. H., "Runoff Curve Numbers from Partial Area Watersheds," *Journal of the Irrigation and Drainage Division*, ASCE, Vol. 105, No. IR4, Proc. Paper 15024, Dec., 1979, pp. 375–389.
5. Hjelmfelt, A. T., Jr., "Empirical Investigation of Curve Number Technique," *Journal of the Hydraulics Division*, ASCE, Vol. 106, No. HY9, Proc. Paper 15693, Sept., 1980, pp. 1471–1476.

6. *National Engineering Handbook*, Section 4, USDA, SCS, Washington, D.C., 1972.
7. "Peak Rates of Discharge for Small Watersheds," *Engineering Field Manual for Conservation Practices*, Chap. 2, Revised for New Mexico, USDA, SCS, Albuquerque, N.M., Oct., 1973, 31 pp.
8. Ragan, R. M., and Jackson, T. J., "Runoff Synthesis Using Landsat and SCS Model," *Journal of the Hydraulics Division*, ASCE, Vol. 106, No. HY5, Proc. Paper 15387, May, 1980, pp. 667–678.
9. "Review and Evaluation of Urban Flood Flow Frequency Procedures," *Bibliographies and Literature of Agriculture*, No. 9, USDA, SEA, Beltsville, Md., Aug., 1980, 63 pp.
10. "Urban Hydrology for Small Watersheds," *Technical Release No. 55*, USDA, SCS, Washington, D.C., Jan, 1975.

Appendix II.—Notation

The following symbols are used in this paper:

CN = SCS runoff curve number;
P = storm rainfall, in inches (cm);
Q = direct storm runoff, in inches (cm);
Q_2/Q_1 = relative runoff; and
S = potential maximum retention, in inches (cm).

Young's Inequality for Three-Dimensional Flows

By Aristides Th. Marinos,[1] A. M. ASCE

Introduction

The numerical treatment of three-dimensional flows in porous media requires a careful approach regarding the stability and computer memory-time characteristics of the method employed. When extensive information about the flow is needed, especially for time dependent flows, the computations can be quite lengthy, and, as far as the author knows, there are no stability criteria of general validity concerning the numerical procedures used. However, in certain cases, one may not be interested in such detailed information, but, in some relations

[1]Computing Center of the Public Power Corp., 3 Agion Apostolon St., Athens 811, Greece.

Note.—Discussion open until May 1, 1982. To extend the closing date one month, a written request must be filed with the Manager of Technical and Professional Publications, ASCE. Manuscript was submitted for review for possible publication on October 15, 1980. This paper is part of the Journal of the Irrigation and Drainage Division, Proceedings of the American Society of Civil Engineers, ©ASCE, Vol. 107, No. IR4, December, 1981. ISSN 0044-7978/81/0004-0388/$01.00.

of general character concerning the principal flow parameters and consequently the use of an elaborated model, detailed information would not be the proper choice. Such a relation is the Young's inequality which, for steady drainage through a porous strip contained between two parallel ditches, relates the height of the water table at its center, the precipitation intensity, the ditch spacing, and the level of permanent water horizon (1).

This note deals with an extension of Young's inequality to three-dimensional flows. Although the extension is formulated with regard to a transient Darcian flow through an anisotropic prismatic porous region surrounded by a peripheral ditch (Fig. 1), its main practical significance seems to be the numerical determination of bounds on the precipitation for steady flows, so that the maximum height of the water table above the impervious boundary will not exceed a

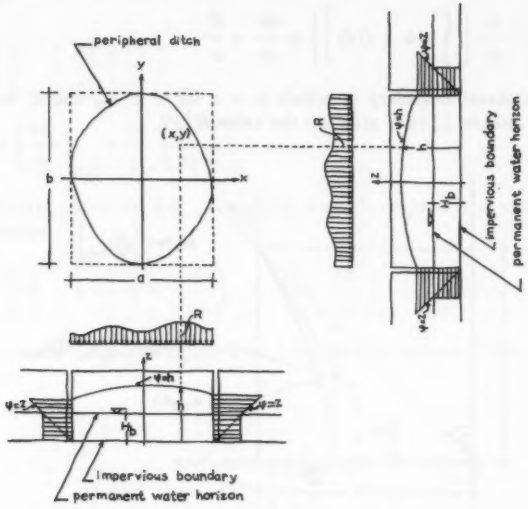

FIG. 1.—Flow Conditions at Time, t

given value. After the general form of the extended Young's inequality has been presented, it is specialized in steady flows in orthotropic regions of rectangular cross section since for this case one can derive closed type formulas for the bounds in question.

Mathematical Analysis

The physical process of the flow, in which s stands for the porosity at the point (x,y,z) of the medium while k_x, k_y, and k_z denote the permeability coefficients with respect to the directions x, y, and z, respectively, is described in Fig. 1. The other symbols, ϕ, h and R, appearing in Fig. 1 have the meaning of velocity potential, height of water table above the impervious boundary,

and precipitation at the point (x,y) at time, t, respectively.

For establishing the extended Young's inequality in the form presented in this note, an additional assumption, regarding k_x, k_y, and s, seems necessary namely that k_x, k_y, and s are functions of x and y only. Since the form of this inequality depends on the quantity, $\int_0^h (\phi - z)\,dz$, which plays a key role in finding for steady flows bounds on R, associated with a maximum height of the water table, the governing pde of $\int_0^h (\phi - z)\,dz$ is first recorded.

After slightly modifying the analysis (2) to take into account the fact that k_x, k_y, and s are not constant and that there is also a time varying precipitation, R, one can prove that the pde in question is

$$\frac{\partial}{\partial x}\left\{\frac{k_x}{s}\cdot\frac{\partial}{\partial x}\left[\int_0^h (\phi - z)\,dz\right]\right\}$$

$$+\frac{\partial}{\partial y}\left\{\frac{k_y}{s}\cdot\frac{\partial}{\partial y}\left[\int_0^h (\phi - z)\,dz\right]\right\} = \frac{\partial h}{\partial t} - \frac{R}{s} \quad \ldots\ldots\ldots\ldots\ldots\ldots (1)$$

At the peripheral boundary in which $\phi = z$ for $z \geqq H_b$ and $\phi = H_b$ for $z \leqq H_b$, the integral $\int_0^h (\phi - z)\,dz$ has the value $H_b^2/2$.

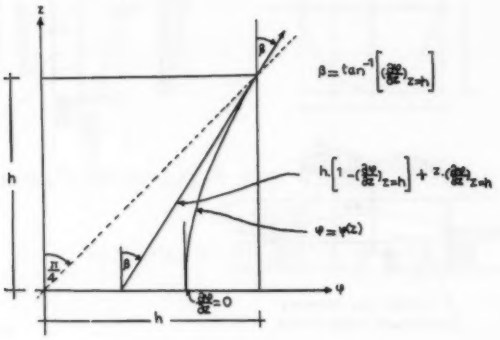

FIG. 2.—Variation of ϕ versus z

Since the derivation of the extended Young's inequality will be based on a geometrical interpretation of an observation related to the physics of the flow, a rough sketch of the variation of ϕ versus z while both x and y are kept constant, is presented in Fig. 2.

The curve of $\phi = \phi(z)$ sketched in Fig. 2, corresponds to the monotonic decrease of the z-component of fluid velocity from $z = h$–$z = 0$, a condition that is considered true for the simple drawdown and recharge problems considered (2). From Fig. 2 it is evident that

$$h \geqq \phi \geqq h\left[1 - \left(\frac{\partial \phi}{\partial z}\right)_{z=h}\right] + z\left(\frac{\partial \phi}{\partial z}\right)_{z=h} \quad \ldots\ldots\ldots\ldots\ldots\ldots (2)$$

$$\text{or} \quad h - z \geqq \phi - z \geqq (h - z)\left[1 - \left(\frac{\partial \phi}{\partial z}\right)_{z=h}\right] \quad \ldots\ldots\ldots\ldots\ldots\ldots (2a)$$

The latest relation is first integrated from $z = 0$–$z = h$ and then the three sides of it are divided by the positive quantity $\int_0^h (\phi - z)\,dz$ so that finally

$$1 \geqq \frac{\int_0^h (\phi - z)\,dz}{\int_0^h (h - z)\,dz} \geqq 1 - \left(\frac{\partial \phi}{\partial z}\right)_{z=h} \quad \ldots\ldots\ldots\ldots\ldots\ldots\ldots\ldots (3)$$

On the other hand, since the relation $h(x,y,t) = \phi\,[x,y,h(x,y,t),t]$ holds, it follows that

$$\frac{\partial h}{\partial x} = \left(\frac{\partial \phi}{\partial x}\right)_{z=h} + \frac{\partial h}{\partial x}\left(\frac{\partial \phi}{\partial z}\right)_{z=h} \quad \ldots\ldots\ldots\ldots\ldots\ldots\ldots\ldots (4)$$

$$\text{and} \quad \frac{\partial h}{\partial y} = \left(\frac{\partial \phi}{\partial y}\right)_{z=h} + \frac{\partial h}{\partial y}\left(\frac{\partial \phi}{\partial z}\right)_{z=h} \quad \ldots\ldots\ldots\ldots\ldots\ldots\ldots\ldots (5)$$

Taking $(\partial\phi/\partial x)_{z=h}$ and $(\partial\phi/\partial y)_{z=h}$ from Eqs. 4 and 5, respectively, and inserting them in relation

$$\frac{\partial h}{\partial x}\left(\frac{k_x}{s}\cdot\frac{\partial \phi}{\partial x}\right)_{z=h} + \frac{\partial h}{\partial y}\left(\frac{k_y}{s}\cdot\frac{\partial \phi}{\partial y}\right)_{z=h} - \left(\frac{k_z}{s}\cdot\frac{\partial \phi}{\partial z}\right)_{z=h} = \frac{\partial h}{\partial t} - R \quad \ldots\ldots (6)$$

which express the conditions satisfied by ϕ on the free surface, it is not difficult to prove that

$$\left(\frac{\partial \phi}{\partial z}\right)_{z=h} = \frac{k_x\cdot\left(\frac{\partial h}{\partial x}\right)^2 + k_y\cdot\left(\frac{\partial h}{\partial y}\right)^2 - s\cdot\frac{\partial h}{\partial t} + R}{k_x\cdot\left(\frac{\partial h}{\partial x}\right)^2 + k_y\cdot\left(\frac{\partial h}{\partial y}\right)^2 + k_z} \quad \ldots\ldots\ldots\ldots (7)$$

The combination of Eqs. 3 and 7 leads immediately to

$$1 \geqq \frac{\int_0^h (\phi - z)\,dz}{\int_0^h (h - z)\,dz} \geqq \frac{k_z - \left(R - s\cdot\frac{\partial h}{\partial t}\right)}{k_x\left(\frac{\partial h}{\partial x}\right)^2 + k_y\left(\frac{\partial h}{\partial y}\right)^2 + k_z} \quad \ldots\ldots\ldots\ldots (8)$$

which constitutes the extended form of Young's inequality to three-dimensional transient flows through prismatic porous regions surrounded by a peripheral ditch. For steady flows and for the point (x,y) which corresponds to the maximum height of water table $(\partial h/\partial x = \partial h/\partial y = 0)$ as well as to $\int_0^h (\phi - z)\,dz = \max$, Eq. 8 takes the form

$$1 \geqq \frac{2\left[\int_0^h (\phi - z)\,dz\right]_{\max}}{h_{\max}^2} \geqq 1 - \frac{R}{k_z} \quad \ldots\ldots\ldots\ldots\ldots\ldots\ldots\ldots (9)$$

In case of a one-dimensional steady flow with constant precipitation, R, through an isotropic medium contained between two parallel ditches of spacing, a, the pde (1) is greatly simplified to

$$\frac{d^2}{dx^2}\left[\int_0^h (\phi - z)\,dz\right] = -\frac{R}{k} \quad \ldots\ldots\ldots\ldots\ldots\ldots\ldots\ldots (10)$$

The solution of the differential Eq. 10 satisfying $\int_0^h (\phi - z)\,dz = H_b^2/2$ at $x = \pm a/2$, is

$$\int_0^h (\phi - z)\,dz = \frac{H_b^2}{2} + \frac{R}{2k}\left(\frac{a^2}{4} - x^2\right) \quad \ldots\ldots\ldots\ldots\ldots\ldots\ldots\ldots (11)$$

After the expression $\int_0^h (\phi - z)\,dz$ at $x = 0$ is inserted in Eq. 9, the latest one is transformed to

$$1 \geqq \frac{H_b^2 + \frac{R}{k}\left(\frac{a}{2}\right)^2}{h_{\max}^2} \geqq 1 - \frac{R}{k} \quad \ldots\ldots\ldots\ldots\ldots\ldots\ldots\ldots (12)$$

which constitutes the already known form of Young's inequality (1). More generally, for steady flows through media of arbitrary cross sections, one can solve by means of the FEM the pde (1) with $\int_0^h (\phi - z)\,dz = H_b^2/2$ at the boundary and for prescribed functional dependences of k_x, k_y, and s on x and y. Since in some cases R may not be constant, the spatial variation of R is supposed to have the form $R = R_{\max} f(x,y)$ with $f(x,y)$ a dimensionless function of x and y (most frequently $f(x,y) = 1$) and $R_{\max}$ equal to the maximum precipitation intensity.

After the values of $\int_0^h (\phi - z)\,dz$ at selected points of the medium's cross section have been calculated, it is possible to determine approximately the position characterized by $\int_0^h (\phi - z)\,dz = \max$ which corresponds to the maximum height $h_{\max}$ of the water table as well. For $R = R_{\max} f(x,y)$ and since $\int_0^h (\phi - z)\,dz$ is constant equal to $H_b^2/2$ at the boundary, it is evident that relation Eq. 9 is equivalent to

$$1 \geqq \frac{H_b^2 + 2\,[G(x,y)]_{\max}}{h_{\max}^2} \geqq 1 - \frac{R_{\max}}{k_z} \cdot \lambda \quad \ldots\ldots\ldots\ldots\ldots\ldots\ldots\ldots (13)$$

in which $G(x,y)$ denotes the solution of Eq. 1 which takes the zero value at the boundary, and λ the value of $f(x,y)$, at the point where the maximum value of $G(x,y)$ has appeared.

Since the function $G(x,y)$ itself is proportional to $R_{\max}$, the above relation can be used in establishing bounds on the maximum precipitation intensity so that the height of water table will not exceed $h_{\max}$.

For doubly symmetric problems, i.e., for regions whose geometrical and physical properties as well as precipitation intensity are distributed along two

axes of symmetry, it is apparent that h_{max} appears at the center of the medium's cross section. For these problems it is possible to apply the FEM to the region's quarter only employing simple triangular elements of the C° class (3).

Example.—Since the main practical use of the extended Young's inequality is the numerical determination of bounds on R so that the height of water table will not exceed a given value, it seems worthwhile to examine a case for which closed type formulas in which these bounds can be found. This example corresponds to steady drainage through an orthotropic region of rectangular cross section with sides a and b (see the dotted rectangle in Fig. 1) and for

TABLE 1.—Variation of $\psi = \psi(\sqrt{k_y/k_x} \cdot a/b)$ versus $\sqrt{k_y/k_x} \cdot a/b$

$\sqrt{k_y/k_x} \cdot a/b$ (1)	ψ (2)	$\sqrt{k_y/k_x} \cdot a/b$ (3)	ψ (4)	$\sqrt{k_y/k_x} \cdot a/b$ (5)	ψ (6)
0.100	0.0125	0.400	0.0480	0.700	0.0686
0.125	0.0156	0.425	0.0504	0.725	0.0695
0.150	0.0187	0.450	0.0527	0.750	0.0703
0.175	0.0219	0.475	0.0549	0.775	0.0710
0.200	0.0250	0.500	0.0569	0.800	0.0716
0.225	0.0281	0.525	0.0588	0.825	0.0721
0.250	0.0311	0.550	0.0606	0.850	0.0726
0.275	0.0341	0.575	0.0623	0.875	0.0729
0.300	0.0371	0.600	0.0638	0.900	0.0732
0.325	0.0400	0.625	0.0652	0.925	0.0734
0.350	0.0427	0.650	0.0664	0.950	0.0736
0.375	0.0454	0.675	0.0675	0.975	0.0736
				1.000	0.0737

constant precipitation, R, i.e., $f(x,y) = 1$. For k_x, k_y, s, and R constants, the pde (1) has the form

$$\left(k_x \cdot \frac{\partial^2}{\partial x^2} + k_y \cdot \frac{\partial^2}{\partial y^2}\right) G(x,y) = -R \quad \ldots\ldots\ldots\ldots\ldots\ldots\ldots\ldots \quad (14)$$

while the solution, $G(x,y)$, satisfying $G(x,y) = 0$, at the boundary, is

$$G(x,y) = \frac{16ab}{\pi^4} \cdot \frac{R}{\sqrt{k_x k_y}} \sum_{i=1}^{\infty} \sum_{j=1}^{\infty} \frac{\dfrac{(-1)^{i+j-2}}{(2i-1)(2j-1)}}{(2i-1)^2 \sqrt{\dfrac{k_x}{k_y} \cdot \dfrac{b}{a}} + (2j-1)^2 \sqrt{\dfrac{k_y}{k_x} \cdot \dfrac{a}{b}}}$$

$$\cdot \cos \frac{(2i-1)\pi x}{a} \cdot \cos \frac{(2j-1)\pi y}{b} \quad \ldots\ldots\ldots\ldots\ldots\ldots\ldots\ldots \quad (14a)$$

Due to the double symmetry of the problem, it is obvious that the maximum value of $G(x,y)$ appears at the center of the region ($x = y = 0$), so that after defining

$$\psi = \psi\left(\sqrt{\frac{k_y}{k_x}} \cdot \frac{a}{b}\right)$$

$$= \frac{16}{\pi^4} \sum_{i=1}^{\infty} \sum_{j=1}^{\infty} \frac{\dfrac{(-1)^{i+j-2}}{(2i-1)(2j-1)}}{(2i-1)^2 \sqrt{\dfrac{k_x}{k_y}} \cdot \dfrac{b}{a} + (2j-1)^2 \sqrt{\dfrac{k_y}{k_x}} \cdot \dfrac{a}{b}} \quad \ldots\ldots\ldots (15)$$

one can set

$$[G(x,y)]_{\max} = ab \cdot \frac{R}{\sqrt{k_x k_y}} \cdot \psi\left(\sqrt{\frac{k_y}{k_x}} \cdot \frac{a}{b}\right) \quad \ldots\ldots\ldots\ldots\ldots (16)$$

In Table 1, values of $\psi(\sqrt{k_y/k_x} \cdot a/b)$ for selected values of the argument $\sqrt{k_y/k_x} \cdot a/b$ are recorded, which were calculated after a simple program in FORTRAN was written.

Using Eq. 16 for $[G(x,y)]_{\max}$ in Eq. 13 and noting that $\lambda = 1$, the latest one takes the form

$$1 \geqq \frac{H_b^2}{h_{\max}^2} + \frac{2ab}{h_{\max}^2} \cdot \frac{R}{\sqrt{k_x k_y}} \cdot \psi\left(\sqrt{\frac{k_y}{k_x}} \cdot \frac{a}{b}\right) \geqq 1 - \frac{R}{k_z} \quad \ldots\ldots\ldots (17)$$

from which bounds on the precipitation intensity can be found.

Conclusion

The main practical significance of the extended Young's inequality seems to be the determination of bounds on the precipitation intensity for steady flows so that the maximum height of water level will not exceed a prescribed value. In most cases, this is made possible after the pde satisfied by $\int_0^h (\phi - z)\,dz$ is solved by means of the FEM and the value of $[\int_0^h (\phi - z)\,dz]_{\max}$ is numerically determined.

For steady drainage through regions of more or less "regular" cross section (e.g. rectangular) and for such a form of precipitation intensity that a formal solution of the pde (1) is possible, closed type formulas for these bounds can be found.

Appendix.—References

1. American Society of Agronomy, *Agronomy*, "Drainage for Agriculture," No. 17, Madison, Wisc., 1974, pp. 212–214.
2. Murray W. A., and Monkmeyer P. L., "Validity of Dupuit-Forcheimer Equation," *Journal of the Hydraulics Division*, ASCE, Vol. 99, No. HY9, Proc. Paper 9997, Sept., 1973, pp. 1573–1583.
3. Rossow, M. L., "Symmetry Conditions in Finite Element Field Problems," *Journal of the Engineering Mechanics Division*, ASCE, Vol. 103, No. EM1, Feb., 1977, pp. 215–218.

Relation Between Curve Number and Runoff Coefficient

By Richard H. McCuen,[1] A. M. ASCE and Timothy R. Bondelid[2]

Introduction

The rational method (1) is probably the one most widely used for estimating peak discharges for inlet designs on small watersheds. The basic input requirements include the drainage area, a rainfall intensity for the design return period, and a runoff coefficient (C). As it is usually applied, the rainfall intensity is for a storm duration equal to the time of concentration, which is dependent on the land use, the watershed slope, and the hydraulic length to the inlet. The runoff coefficient is most often obtained from a table as a function of land use, with the table providing a range of values for each land use. While not used widely, tables of recommended C values exist that allow for variation in C with respect to soil type, rainfall intensity, slope, design frequency, and surface roughness (3). When a range of values is given for a particular land use, it is assumed that the larger values of the runoff coefficient should be used for the larger events (i.e., return periods greater than 25 yr) and large slopes; however, the tables often lack sufficient detail on exactly what value should be used in any given case.

The Soil Conservation Service TR-55 graphical method (2,4) is another widely used technique for estimating peak discharges for small drainage areas. Input includes the drainage area, the 24 hr precipitation depth for the design return period, the runoff curve number, and the time of concentration. The runoff curve number (CN) is an index of runoff potential and is a function of the soil type and land use, the soil cover complex and condition, and the antecedent soil moisture. In design, the antecedent soil moisture adjustment usually is not used to change the input value of the CN.

In general, it is evident that the two methods, the rational formula and the TR-55 graphical method, are based on the same input data: drainage area, a rainfall index, the time of concentration, and a runoff index. Therefore, it may be of interest to examine the relationship between the methods. The objective of this study is to demonstrate that the two runoff indices (i.e., the curve number and the runoff coefficient) are related.

[1]Assoc. Dean, Coll. of Engrg., Univ. of Maryland, College Park, Md.
[2]Grad. Research Asst., Dept. of Civ. Engrg., Univ., of Maryland, College Park, Md.

Note.—Discussion open until May 1, 1982. To extend the closing date one month, a written request must be filed with the Manager of Technical and Professional Publications, ASCE. Manuscript was submitted for review for possible publication on April 23, 1981. This paper is part of the Journal of the Irrigation and Drainage Division, Proceedings of the American Society of Civil Engineers, ©ASCE, Vol. 107, No. IR4, December, 1981. ISSN 0044-7978/81/0004-0395/$01.00.

Relation Between Runoff Indices

The two runoff indices, the rational C and the SCS CN, are, for numerous reasons, important input parameters. First of all, and probably foremost, estimated peak discharges are very sensitive to these indices and any errors in an estimated value will appear as an error in the estimated peak discharge. Secondly, a comparison between C and CN may reveal differences in the rationality of the two models. Thirdly, both models lack an extensive empirical validation. The internal validity of the rational method has been questioned by many. Thus, a comparison of the two methods may identify potential sources of bias or some imprecision of the two methods. This would be especially useful to a regulatory agency that is contemplating a change in policy that would require one method to be used in place of the other. Fourth of all, this analysis would be useful when design policies are at odds, with the policy of one agency requiring use of one method and another agency requiring designs using the other method. The relationship between C and CN then could be used to adjust the C (or CN) table so that inconsistent design estimates could be avoided. Fifthly, the relationship would be of value in evaluating policies concerning the use of different methods for different size watersheds. For example, in Maryland SCS methods are recommended for most analyses but the rational formula is permitted for inlet areas less than 5 acre. An analysis of the relationship between C and CN would be useful in identifying significant discrepancies in design peak discharges at the drainage area "break point" (i.e., the 5 acre limit). Sixth of all, the two methods use different land use category systems. In some cases, a designer may select one method over another because of the presentation of the land use data; also, the C versus CN relationship may be helpful in refining land use categories to eliminate inconsistencies in design due solely to vague land use descriptions.

The rational formula is given by

$$Q = CiA \quad \ldots\ldots\ldots\

from a graph of q_u versus the time of concentration, in hours (4); this graph can be represented by an exponential relationship over small ranges of the time of concentration:

$$q_u = b_o t_c^{b_1} \quad \ldots \quad (5)$$

in which b_o and b_1 = fitting coefficients. Similarly, the rainfall intensity of Eq. 1 can be represented by an exponential relationship:

$$i = d_o t_c^{d_1} \quad \ldots \quad (6)$$

in which d_o and d_1 = fitting coefficients.

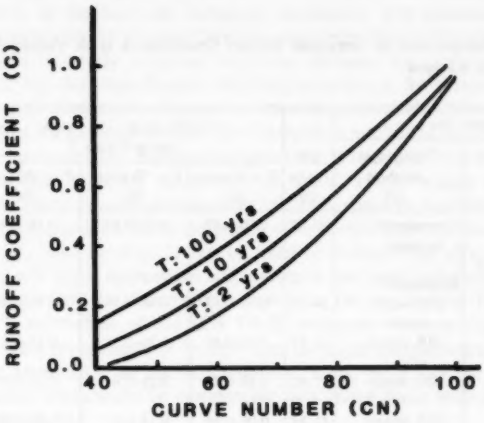

FIG. 1.—Relationship between Runoff Coefficient and Curve Number for Baltimore, Md.

If the two methods are assumed to be equally accurate and to provide the same true value of the peak discharge, then the following equality is obtained from the above equations:

$$C(d_o t_c^{d_1})\, A = (b_o t_c^{b_1}) \left(\frac{A}{640}\right) \left[\frac{(P - 0.2S)^2}{P + 0.8S}\right] \quad \ldots \quad (7)$$

Solving for C yields

$$C = \frac{b_o t_c^{b_1}}{640\, d_o t_c^{d_1}} \left[\frac{(P - 0.2S)^2}{P + 0.8S}\right] \quad \ldots \quad (8)$$

Since S is a function of the CN, then the relation between C and CN can be obtained for any design frequency, location, and time of concentration. Values for b_o and b_1 are a function only of the time of concentration, while d_o and d_1 vary with the design frequency, location, and the time of concentration.

Using rainfall intensity-duration-frequency data for Baltimore, Md., and times

of concentration up to two hr, Eq. 8 was solved for return periods (T) of 2, 10, and 100 yr; the resulting values are shown graphically in Fig. 1. The variation due to a change in time of concentration was very small in comparison with the change in return period, and thus the curves of Fig. 1 are adequate for all times of concentration less than 2 hr. The curves of Fig. 1 were used to estimate the runoff coefficient for the range of curve numbers across soil groups. Table 1 shows the land use categories usually used for the rational method and the Soil Conservation Service land use category that most closely approximates them. The CNs for soil groups *A* and *D* are given as the CN range. These values are used to estimate a range of runoff coefficients from Fig. 1. Frequently used values of *C* are also shown. For some land uses, the

TABLE 1.—Comparison of Accepted Runoff Coefficients with Values Estimates for Curve Number Ranges

Land Use		CN range (3)	C Values for CN Range Using Figure 1			Accepted C values (7)
Rational method (1)	Graphical method (2)		T = 2 years (4)	T = 10 years (5)	T = 100 years (6)	
Business	Commercial/ business	89–95	0.70–0.87	0.77–0.90	0.86–0.96	
Downtown						0.70–0.95
Neighborhood						0.50–0.70
Residential	Residential					
Single-family	25% impervious	54–85	0.08–0.62	0.18–0.69	0.32–0.79	0.30–0.50
Multi-units (detached)	38% impervious	61–87	0.16–0.66	0.26–0.73	0.42–0.82	0.40–0.60
Multi-units (attached)	65% impervious	77–92	0.43–0.79	0.53–0.84	0.66–0.91	0.60–0.75
Residential (suburban)	20% impervious	51–84	0.06–0.59	0.14–0.66	0.28–0.78	0.25–0.40
Industrial	Industrial	81–93	0.52–0.82	0.61–0.86	0.73–0.93	
Light						0.50–0.80
Heavy						0.60–0.90
Parks, cemeteries	Open space (good condition)	39–80	0.00–0.49	0.04–0.58	0.12–0.71	0.10–0.25
Playgrounds	Open space (fair condition)	49–84	0.04–0.59	0.12–0.66	0.25–0.78	0.20–0.35

two methods agree quite closely on runoff potential. For example, the commercial/business CN values range from 89–95, which corresponds to C values of 0.70–0.96 over the three return periods. The accepted C values for downtown business areas range from 0.70–0.95.

Similarly, close values result for the industrial land use category. However, some land use categories show significant differences. For open space such as parks, cemeteries, and playgrounds, the CN range results in a much wider variation in C values than the recommended C values. This may reflect different levels of impervious area associated with different specific uses within the open space category. The residential land use categories also show significant variation. This may be the result of the difficulty in associating land use categories. The

residential land use separation for the rational method is too vague in that one reasonably can expect larger differences in runoff potential for single-family residential areas than would be suggested by accepted C values (6). Thus, the TR-55 separation would be preferable.

Conclusions

In conclusion, the two peak discharge design methods are based on similar input data and, thus, represent design alternatives; therefore, a comparison is in order. The analysis of the relationship provides several conclusions: The two methods appear to give similar peak discharge estimates when one can find agreement in the land use category separation. For regulatory agencies involved in specifying the rational formula, it appears that consistency of design estimates could be vastly improved by better defining the land use categories and by identifying the other factors affecting variation in the runoff coefficient.

Secondly, peak discharge estimates by the rational formula are more sensitive to C values than are estimates by the TR-55 graphical method to the CN, especially for the larger return periods. Increased imprecision that results from this sensitivity can be controlled by better delineation of the C values within the range of values in the tables. In comparison with tables commonly available, the tables by Rossmiller (3) provide a better definition of C values. The relationship between C and CN, provided by Fig. 1, can be used to indicate the effects on C due to changes in soil type, antecedent soil moisture, and land use condition.

In addition the graphical method is based on the conceptual framework of the RUNOFF subroutine of the SCS TR-20 computer program (5); it provides a very reasonable approximation except when the initial abstraction is significantly greater than about 25% of the precipitation. Thus, peak discharges from the rational formula also should be comparable with those made with the RUNOFF subroutine of TR-20.

Fourthly, the C values of Table 1, estimated from the CN values, are characterized by much higher variation than the accepted C values. This results in part because of the disparity in land use categories. However, in many cases, the upper CN value results in a wide disparity between the estimated and accepted C values. This partially represents a difference in the conceptual basis of the model and would indicate that there would be a systematic bias in peak discharges estimated with the two models. When design projects are controlled by different policies (e.g., watershed size limitations, county or state boundaries), this source of bias should be recognized and handled in a systematic manner. In general, it appears that for residential and open space land use categories the graphical method will provide higher peak discharge estimates than the rational method. At the very least, the relationship can be used to adjust C values for storm frequency and soil type; such adjustments may reduce inconsistency in estimates.

It also appears that the effect of locational differences in C values could be assessed by evaluating the relationship for locations other than Baltimore; however, an initial analysis shows that location is a minor factor, and the results for other locations will be quite similar.

And finally, the SCS methods, including the TR-55 graphical method, are often criticized because they are based on a 24 hr storm distribution. The results of this analysis indicate that this assumption does not introduce a bias into

the estimated peak discharge; for those familiar with the way in which the SCS storm distributions are constructed, the lack of a bias is rational.

Appendix.—References

1. ASCE and Water Pollution Control Federation, *Design and Construction of Sanitary and Storm Sewers*, ASCE Manual No. 37, New York, N.Y., 1969.
2. McCuen, R. H., *A Guide to Hydrologic Analysis Using SCS Methods*, Prentice-Hall, Inc., Englewood Cliffs, N.J., 1981.
3. Rossmiller, R. L., "The Rational Formula Revisited," *Proceedings*, International Symposium on Urban Storm Runoff, University of Kentucky, Lexington, Ky., 1980.
4. Soil Conservation Service, *Urban Hydrology for Small Watersheds, Technical Release No. 55*, U.S. Department of Agriculture, Jan., 1975.
5. Soil Conservation Service, *Computer Program for Project Formulation: Hydrology, Technical Release 20*, U.S. Department of Agriculture, 1965.
6. Whipple, W., Jr., DiLovie, J. M., and Pytlar, T., Jr., "Erosional Potential of Streams in Urbanizing Areas," *Water Resources Bulletin*, Vol. 17, No. 1, 1981, pp. 36–45.

Irrigation Practices for Reclaimed Alkali Soils

By V. V. Dhruva Narayana[1] and N. K. Tyagi[2]

Introduction

Alkali soils, about 2,500,000 ha, of the Indo-Gangetic alluvial plains are characterized by impermeable surface soils and hydraulically impeded subsurface horizons. This mainly is due to the high exchangeable sodium (pH 10.4) present in them. These areas are now being reclaimed by farmers on a large scale by land levelling and field bunding, applying gypsum (as an amendment), and by cultivating rice (June–October) and wheat (November–April) in rotation (1,4).

A survey of the irrigation practices adopted by the farmers of the area revealed that more than 70% of them obtain their irrigation by pumping the good quality ground water (EC = 600 micromhos/cm) and applying an average of about 150 and 60 cm for rice and wheat, respectively, in comparison, with 100 and

[1]Sci.-S_4, Div. of Engrg., Central Soil Salinity Research Inst., Karnal-132001, Haryana, India.

[2]Sci.-S_2, Div. of Engrg., Central Soil Salinity Research Inst., Karnal-132001, Haryana, India.

Note.—Discussion open until May 1, 1982. To extend the closing date one month, a written request must be filed with the Manager of Technical and Professional Publications, ASCE. Manuscript was submitted for review for possible publication on April 15, 1981. This paper is part of the Journal of the Irrigation and Drainage Division, Proceedings of the American Society of Civil Engineers, ©ASCE, Vol. 107, No. IR4, December, 1981. ISSN 0044-7978/81/0004-0400/$01.00.

45 cm applied at the research farm of the Central Soil Salinity Research Institute (CSSRI), Karnal. Thus, there seems to be considerable scope for improving irrigation efficiencies in the farmers' fields.

Objectives

Reclaimed alkali soils require light and more frequent irrigations for wheat crop (2). The farmers do not provide any flow regulating devices to meet this

FIG. 1.—Sloping Borders for Wheat Crop

FIG. 2.—Compartmentalized Sloping Borders for Rice Crop

requirement. This can, therefore, only be satisfied by minimizing the application times through selection of proper dimensions (length and width) of the border strips (Fig. 1) and cutting off the stream when it has advanced adequately in the border. Another possibility is to adopt a sloping border instead of a level one. The sloping border can also be adopted to rice cultivation by

compartmentalization or segmentation (Fig. 2). These ideas were evaluated in a series of three field experiments at CSSRI during 1975–78 with the following objectives: (1) Comparison of graded and level borders; (2) Determination of the stream cutoff point; (3) Determination of the optimum border dimensions; and (4) Adoption of sloping borders for rice cultivation.

Details of Experiments

Experiment No. 1 (1975-76, 1976-77).—Level and graded borders:

Length, L—90 m.

Width, W—5 m.

Slope, S—A level border and a border with 0.1% (the prevailing natural slope, just smoothed on the surface).

Irrigation cutoff, C_R—Four cutoff treatments, viz. when the stream has advanced to 55%, 70%, 85%, and 100% of the total length of the border.

Irrigation depth—The irrigation depth, D, in cm in each irrigation is computed from the application time and stream discharge.

Stream discharge—A constant discharge of 10 Lps (as obtained normally in the farmers' fields) was maintained during each irrigation by a regulatory valve. A Parshall flume was installed below the valve for measurement of discharge.

Irrigation interval, in days.—If D cm were the depth of the previous irrigation,

TABLE 1.—Irrigation Efficiencies and Wheat Crop Yield in Graded and Level Borders with Different Cut-off Ratios*

Particulars	Level Border				Graded Border, in Tenths of a Percent			
Cut-off ratios (1)	0.55 (2)	0.70 (3)	0.85 (4)	1.00 (5)	0.55 (6)	0.70 (7)	0.85 (8)	1.00 (9)
Total irrigation water applied, in centimeters	33.9	35.4	37.4	38.6	26.1	28.5	28.7	31.5
Portion of the border covered in each irrigation, as a percentage	61	77	91	100	85	100	100	100
Number of irrigations	7	6	5	4	7	6	6	5
Application efficiency, as a percentage	67	56	53	48	86	84	80	63
Distribution efficiency, as a percentage	29	53	60	70	64	89	72	71
Crop yield, in quintals per hectare	28.4	31.3	32.5	30.7	31.8	38.5	37.9	36.4
Water use efficiency, in kilograms per hectare per centimeter	87.7	88.8	92.1	83.0	119.3	135.8	132.5	117.9

*Average values for both years of the study.

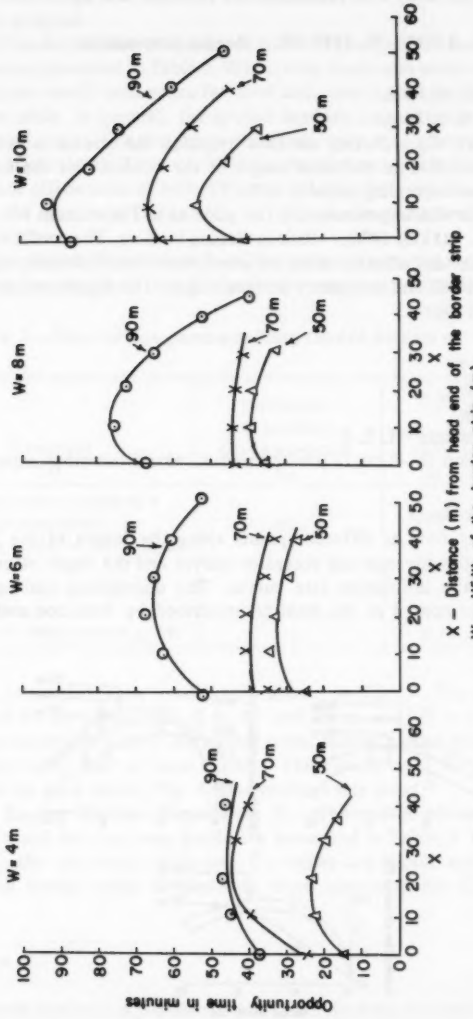

FIG 3.—Variation of Opportunity Time in Different Sized Borders

the next irrigation will be due after an interval of 't' days, during which the cumulative pan evaporation E (in cm) is equal to $D/0.7$ (8). If there is any rainfall during this period, this amount was added to D.

Crop—Wheat (S-1553) with recommended fertilizer and agronomic practices (1).

Experiment No. 2 (1976-77, 1977-78).—Border dimensions:

Length, L—50, 70, 90 m.
Width, W—4, 6, 8, 10 m.

Irrigation cutoff, C_R.—During the first irrigation the stream is cutoff when it has advanced to 85% of the total length of the border. For the subsequent irrigations, the corresponding value is 70%.

Other details for this experiment are the same as in Experiment No. 1.

Experiment No. 3 (1975, 1976).—Rice in sloping borders. The conflicting layout requirements of rice and wheat rotation are attempted to be resolved by segmenting the borders with small and temporary earthen ridges. The segments are interconnected with small pipes:

Length, L—93 m.
Width, W—8 m.
Slope, S—0–1%.
Number of segments—1, 2, 3.
Average Irrigation D—8 cm (a predetermined value from other experiments).

Experimental Procedures

The opportunity time at different points along the length of the border is determined from the advance and recession curves and the depth of cumulative infiltration from the infiltration rate curves. The distribution and application efficiencies are computed in the manner prescribed by Israelson and Hansen

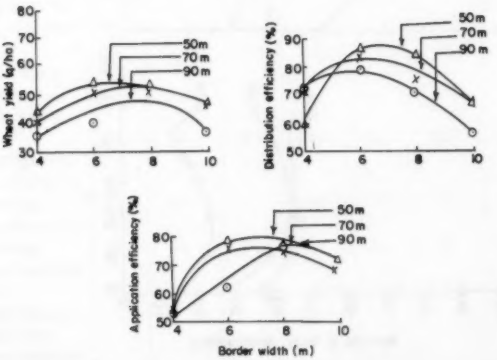

FIG. 4.—Variation of Irrigation Efficiencies and Wheat Crop Yields in Different Sized Borders

(3). Evaluation of the effects of segmenting the border strips on the rice crop was done by computing the uniformity of ponding $Uc = LS/2nD$ (6). In all three experiments, crop yields were recorded to study the crop responses.

Results and Analyses

Level and Graded Borders (Experiment 1).—Data on application and distribution efficiencies are presented in Table 1. Wheat crop yields and water use efficiencies under different cutoff treatments for level and graded borders also are included in the same table. In general, the graded borders are relatively more efficient than the level ones. The irrigation data and crop responses also show that the graded border with 70% cutoff gives the highest application, distribution, and water use efficiencies of 84%, 89% and 135.8 kg/ha/cm. The corresponding values for the best level border ($C_R = 0.85$) in the study are 53%, 60% and 92.1 kg/ha/cm.

Border Dimensions (Experiment 2).—The values of opportunity time at selected points along the length of the border strip, computed from the advance and

TABLE 2.—Effect of Compartmentalizing Graded Borders on Rice Yields

Treatment (1)	Uniformity of ponding *Uc*, as a percent (2)	Rice Yield, in quintals per hectare	
		1975 (3)	1976 (4)
T_1—Sloping border treated as a single compartment.	42	61.8	63.2
T_2—Sloping border in two compartments.	71	64.8	65.4
T_3—Sloping border in three compartments.	81	71.0	67.7
Coefficient of determination at 5%	—	6.1	4.3

recession curves for each border, are shown in Fig. 3. The relationships in the case of border strips with $L = 50$ and 70 m, and $W = 6$ and 8 m (Fig. 3) are represented by nearly horizontal lines, indicating the relative uniformity of the opportunity time in these borders. The variations of the mean efficiency values and the crop yields (Fig. 4) also confirm this trend.

Rice in Sloping Borders (Experiment 3).—The values of the uniformity of ponding *Uc* and the rice crop yields are presented in Table 2. The results have shown that the rice crop yields and *Uc* values are significantly higher at the 5% level in border strips divided into three compartments (T_3) as compared with T_1.

Conclusions

From these studies it is possible to draw the following conclusions with respect to the irrigation practices for growing rice and wheat in alkali soils:

1. A layout of closed and graded borders can be adopted for rice and wheat

rotation. The prevailing gentle land slope of 0.1–0.2% can be immediately adopted as the border grade. There is no need to attempt for absolute level plots and only surface smoothing is sufficient.

2. Light and frequent irrigations can be applied by cutting off the irrigation when it has advanced to 70% of the border length.

3. In farmers' fields, irrigation efficiencies can be improved by adopting graded borders (the prevailing grade of 0.1–0.2%) with lengths in the range of 50–70 m and widths of 6–8 m. These dimensions are particularly suited to small farms, which are common in the region.

4. During the rainy season, rice also can be grown in these graded borders by dividing them into two or three compartments connected by asbestos pipes.

Appendix.—References

1. Abrol, I. P., Dargan, K. S., and Bhumbla, D. R., "Reclaiming Alkali Soils," Bulletin No. 2, Central Soil Salinity Research Institute, 1973, Karnal, India.
2. Gaul, B. L., Abrol, I. P., and Dargan, K. S., "Frequent and Light Irrigation Best for Saline Sodic Soils," *Indian Farming*, Volume 23, No. 4, 1973, pp. 14–15.
3. Israelson, O. W., and Hansen, V. E., *Irrigation Principles and Practices*, John Wiley & Sons. Inc., New York, N.Y., 1967.
4. Narayana, V. V. Dhruva, "Rainwater Management for Low Land Rice Cultivation in India," *Journal of the Irrigation and Drainage Division*, ASCE, Vol. 105, No. 1, 1979, pp. 87–98.
5. Narayana, V. V. Dhruva, Kalra, V. D., and Singh, O. P., "Design of a Farm Layout for Irrigation with Limited Discharges," *Agricultural Water Management* Vol. 3, No. 2, pp. 143–151.
6. Pandey, R. N., Narayana, V. V. Dhruva, Tyagi, N. K., and Gupta, S. K., "Management of Sloping Borders for Rice Cultivation in Alkali Soils," *Indian Journal of Agricultural Sciences*, Vol. 47, No. 12, 1977, pp. 613–616.
7. Tyagi, N. K., "Some Design Aspects of Ponded Borders with Cut Back Stream in Alkali Soils," *Current Agriculture*, Vol. 2, Nos. 1, 2, 1978, pp. 13–16.
8. Tyagi, N. K., and Narayana, V. V. Dhruva, "Evaluation of some On-farm-Water Management Constraints in Surface Irrigation Systems," ICID Bulletin, International Commission on Irrigation and Drainage, New Delhi, India.

Delayed Drainage in a Stream-Aquifer System

By Shlomo P. Neuman[1]

Introduction

In a recent paper published in this journal, Higgins (5) considered the problem of nonsteady flow from an unconfined aquifer into a fully penetrating stream in which the water level fluctuates in a prescribed fashion. He was able to derive approximate analytical expressions for drawdown at any point in the aquifer by assuming that the aquifer material is rigid, the water is incompressible, and the water table is a moving material boundary. To check the validity of his theoretical expressions, Higgins conducted a laboratory experiment with the aid of a sand box. The experimental results were in agreement with theory for the case where the water level in the stream declined linearly with time. However, when the water level in the stream was lowered instantaneously to its final position, the experimental drawdown of the water table at early time was higher than that predicted by theory; at large values of time, some of the experimental water table drawdowns were less than those predicted by theory. Higgins attributed this lack of correspondence between experiment and theory to a failure on the part of his theory to account for unsaturated flow above the water table.

The purpose of this note is to develop an alternative theory which does not account for unsaturated flow and yet, is able to explain Higgins' experimental results. The proposed theory is similar to that of Higgins, with two important exceptions: (1) The aquifer material is assumed to be elastic and the water compressible; and (2) the aquifer is taken to be anisotropic. Whereas Higgins' theory can be viewed as a two-dimensional version of the well-flow problem reported by Boulton (2), the new theory described here derives from the concept of delayed drainage as applied to the problem of unconfined flow to a well by Neuman (6,7).

Theory

Consider an unconfined aquifer of infinite lateral extent resting on an impermeable horizontal layer, such as that shown schematically in Fig. 1. The aquifer material is uniform but anisotropic with principal permeabilities oriented parallel

[1]Prof., Dept. of Hydrology and Water Resources, University of Arizona, Tucson, Ariz. 85721.

Note.—Discussion open until May 1, 1982. To extend the closing date one month, a written request must be filed with the Manager of Technical and Professional Publications, ASCE. Manuscript was submitted for review for possible publication on December 4, 1980. This paper is part of the Journal of the Irrigation and Drainage Division, Proceedings of the American Society of Civil Engineers, ©ASCE, Vol. 107, No. IR4, December, 1981. ISSN 0044-7978/81/0004-0407/$01.00.

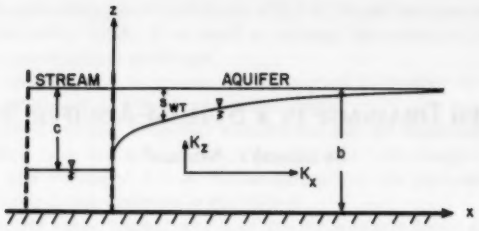

FIG. 1.—Scheme of Stream-Aquifer System

to the coordinates. The aquifer is completely penetrated by a stream of infinite length. Initially, the system is in a static equilibrium, the water level in the stream being at the same elevation as the horizontal water table in the aquifer. At time, $t = 0$, the water level in the stream is suddenly lowered to a new position lying a distance, c, below the original one. As a result of the hydraulic gradient generated by this drop in the water level, water is released from storage in the aquifer due to three mechanisms: compaction of the aquifer material, expansion of the water, and gravity drainage at the free surface.

In analogy to Neuman (6), the problem can be expressed mathematically to a first degree of approximation as

$$\frac{\partial^2 s}{\partial x^2} + K_D \frac{\partial^2 s}{\partial z^2} = \frac{S_s}{K_x} \frac{\partial s}{\partial t}; \quad 0 < z < b \quad \ldots \quad (1)$$

$$s(x, z, 0) = 0 \quad \ldots \quad (2)$$

$$s(0, z, t) = c \quad \ldots \quad (3)$$

$$s(\infty, z, t) = \frac{\partial s}{\partial x}(\infty, z, t) = 0 \quad \ldots \quad (4)$$

$$\frac{\partial s}{\partial z}(x, 0, t) = 0 \quad \ldots \quad (5)$$

$$\frac{\partial s}{\partial z}(x, b, t) = -\frac{S_y}{K_z} \frac{\partial s}{\partial t}(x, b, t) \quad \ldots \quad (6)$$

in which s = drawdown, $K_D = K_z / K_x$; K_z = vertical permeability, K_x = horizontal permeability; S_s = specific (elastic) storage; x = horizontal coordinate; z = vertical coordinate; t = time, b = initial saturated thickness; and S_y = specific yield (drainage porosity). After applying Laplace and infinite sine transforms to Eqs. 1–6, the resulting one-dimensional problem is easily solved. Application of the inverse sine transform together with Mellin's inversion formula in the manner outlined by Neuman (6) leads to the following solution

$$s(x, z, t) = \frac{4c}{\pi} \int_0^\infty y \sin(y\beta^{1/2}) \sum_{n=0}^{\infty} u_n(y)\, dy \quad \ldots \quad (7)$$

$$u_o(y) = \frac{\{1 - \exp[-t_s\beta(y^2 - \gamma_o^2)]\}\cosh(\gamma_o z_D)}{\left[y^2 + (1+\sigma)\gamma_o^2 - \dfrac{(y^2 - \gamma_o^2)^2}{\sigma}\right]\cosh(\gamma_o)} \quad \ldots\ldots\ldots\ldots (8)$$

$$u_n(y) = \frac{\{1 - \exp[-t_s\beta(y^2 + \gamma_n^2)]\}\cos(\gamma_n z_D)}{\left[y^2 - (1+\sigma)\gamma_n^2 - \dfrac{(y^2 + \gamma_n^2)^2}{\sigma}\right]\cos(\gamma_n)}; \quad n \geq 1 \quad \ldots\ldots\ldots (9)$$

and the terms γ_o and γ_n are the roots of the equations

$$\sigma\gamma_o \sinh(\gamma_o) - (y^2 - \gamma_o^2)\cosh(\gamma_o) = 0; \quad \gamma_o^2 < y^2 \quad \ldots\ldots\ldots\ldots (10)$$

$$\sigma\gamma_n \sin(\gamma_n) + (y^2 + \gamma_n^2)\cos(\gamma_n) = 0; \quad n \geq 1;$$

$$(2n-1)\frac{\pi}{2} < \gamma_n < n\pi \quad \ldots\ldots\ldots\ldots\ldots\ldots\ldots\ldots (11)$$

Here $t_s = K_x t/S_s x^2$; $\beta = K_D x_D^2$; $x_D = x/b$; $z_D = z/b$; and $\sigma = S_s b/S_y$.

Behavior at Small and Large Values of Time

If there is no gravity drainage ($S_y = 0$) the aquifer is artesian and $\sigma \to \infty$. Note that $\sigma \to \infty$ can also be interpreted to mean $S_s b \to \infty$, and, thus, $t_s \to 0$, or small values of dimensionless time when $S_y \neq 0$. According to Eqs. 8 and 10, $\sigma \to \infty$ implies $\gamma_o \to 0$ and $\sigma\gamma_o^2 \to y^2$ so that $u_o(y) \to [1 - \exp(-t_s\beta y^2)]/y^2$, whereas Eqs. 9 and 11 show that $u_n(y) \to 0$ for all $n \geq 1$. This together with formula from Gradshteyn and Ryzhik (4) and Abramowitz and Stegun (1) yields

$$s(x,t) = c\,\mathrm{erfc}\,(4t_s)^{-1/2} \quad \ldots\ldots\ldots\ldots\ldots\ldots\ldots\ldots (12)$$

which is identical with a solution developed earlier by Stallman (3) for a confined aquifer.

For large values of t_s, one can follow an argument identical to that of Neuman (7) to show that

$$s(x,t) = c\,\mathrm{erfc}\,(4t_{sy})^{-1/2} \quad \ldots\ldots\ldots\ldots\ldots\ldots\ldots\ldots (13)$$

in which $t_{sy} = K_x bt/(S_s b + S_y)x^2$. Note that in both cases, s is independent of z.

Reduction to Higgins' Solution.—When $S_s = \sigma = 0$, Eq. 8 implies $\gamma_o^2 = y^2$ and $(y^2 - \gamma_o^2)/\sigma = y\tanh(y)$, whereas according to Eq. 9, $u_n(y) = 0$ for all $n \geq 1$. Thus, Eq. 7 reduces to

$$s(x,z,t) = \frac{2c}{\pi}\int_0^\infty \frac{\sin(y\beta^{1/2})}{y}\,\frac{\{1 - \exp[-t_s\beta y\tanh(y)]\}\cosh(yz_D)}{\cosh(y)}\,dy \quad \ldots\ldots (14)$$

which is an extension of Higgins' (5) equation for the case of an anisotropic aquifer. According to Higgins, the solution for an isotropic aquifer at small values of time can be written (in our notation) as

$$s(x,b,t) = \frac{2c}{\pi}\tan^{-1}(t_s x_D) \quad \ldots\ldots\ldots\ldots\ldots\ldots\ldots\ldots (15)$$

in which $t_y = K_z bt/S_y x^2$. At large values of time, Eq. 14 takes on the simple form

$$s(x,t) = c \operatorname{erfc}(4t_y)^{-1/2} \quad \ldots\ldots\ldots\ldots\ldots\ldots\ldots\ldots\ldots\ldots \quad (16)$$

Explanation of Higgins' Experimental Results.—It will be recalled that at small values of time, the water table drawdowns observed experimentally by Higgins (5) exceeded those predicted by his theory. As an example, let us consider his experiment which corresponds to $x_D = 0.33$; $b = 0.48$ m; and $S_y = 0.3$. From his table we find that $s_{WT}/c = 0.16$ at $t_y x_D^2 = 0.017$ and $s_{WT}/c = 0.50$ at $t_y x_D^2 = 0.030$ in which s_{WT} = drawdown of the water table. Eq. 15 due to Higgins underestimates these values, yielding $s_{WT}/c = 0.03$ for $t_y x_D^2 = 0.017$ and $s_{WT}/c = 0.057$ for $t_y x_D^2 = 0.030$. However, if instead of Eq. 15 we use our own Eq. 12 with $\sigma = 0.2$, we calculate $s_{WT}/c \simeq 0.16$ for $t_y s_D^2 = 0.017$ and $s_{WT}/c \simeq 0.30$ for $t_y x_D^2 = 0.030$, both of which are much closer to the experimental results. The relatively large magnitude of σ required in order to fit Eq. 12 to the data may be due to the presence of air bubbles and dissolved air in the water (7).

At large values of time, some of the water table drawdowns observed by Higgins were less than those predicted by his theory. This can be explained simply by the fact that $t_{sy} < t_y$, and, therefore, Eq. 16 due to Higgins will generally give smaller values of s/c than our Eq. 13. With this, it is easy to understand why most of Higgins' data lie above the dashed line, and some (including all black dots) lie above the solid line at large t.

Appendix.—References

1. Abramowitz, M., and Stegun, I. A., eds., *Handbook of Mathematical Functions*, National Bureau of Standards, Applied Math Series 55, Washington, D.C., 1964.
2. Boulton, N. S., "The Drawdown of the Water Table under Nonsteady Conditions near a Pumped Well in an Unconfined Formation," *Proceedings*, Institution of Civil Engineers, London, England, Vol. 3, Part 3, 1954, pp. 564–567.
3. Ferris, J. G., et al., "Theory of Aquifer Tests," *United States Geological Survey Water-Supply Paper*, U.S. Geological Survey, 1536-E, Washington, D.C., 1962, p. 126.
4. Gradshteyn, I. S., and I. M. Ryzhik, *Table of Integrals, Series, and Products*, Academic Press, New York, N.Y., 1965.
5. Higgins, D. T., "Unsteady Drawdown in 2-D Water Table Aquifer," *Journal of the Irrigation and Drainage Division*, ASCE, Vol. 106, No. IR3, Proc. Paper 15696, Sept., 1980, pp. 237–251.
6. Neuman, S. P., "Theory of Flow in Unconfined Aquifers Considering Delayed Response of the Water Table," *Water Resources Research*, Vol. 8, No. 4, 1972, pp. 1031–1045.
7. Neuman, S. P., "Perspective on 'Delayed Yield'," *Water Resources Research*, Vol. 15, No. 4, 1979, pp. 899–908.

Simple Equations for Hooghoudt Equivalent Depth

By John G. Sakkas[1] and Vassilios Z. Antonopoulos[2]

Introduction

Due to its simplicity and relative accuracy as compared with other more elaborate and hence more complicated methods, the Hooghoudt solution to the drainage design problem (1) is widely used by the practicing engineer. In addition, it is the notion of equivalent depth that Hooghoudt introduced, which makes his analysis more important. The equivalent depth has gained considerable significance in the treatment of the transient drainage problem based on the Dupuit-Forchheimer theory (2,4).

In a previous paper by the senior writer (3), the solution to the so-called Hooghoudt equations was generalized by the introduction of dimensionless variables. Application to practice for design purposes was facilitated by the preparation of unique nomographic solutions both for the equivalent depth and the drain spacing formulas. For calculations on a computer in solving transient flow problems, the computation of the equivalent depth requires the storage in the computer memory of an appreciable size table (maximum 300 values).

For a faster determination of the equivalent depth, and to avoid storage of a table in the computer memory, approximate formulas have been introduced (2). Moody's work was based on Hooghoudt's original work. After the detailed reworking of the solution of Hooghoudt equations (3), it was considered appropriate to proceed with finding simple algebraic equations which approximate the equivalent depth in a more satisfactory way. This is the subject of the present note.

Previous Relevant Work.—In the previously mentioned paper (3), the Hooghoudt equations for computing the equivalent depth and drain spacing were given in dimensionless form as follows:

$$\delta = \frac{\sigma}{8(\phi_1 + \phi_2)}; \quad \ldots \quad (1a)$$

$$\sigma^2 = 4\kappa_1\eta^2 + 8\kappa_2\delta\eta \quad \ldots \quad (1b)$$

[1]Prof., School of Engrg., Democritus Univ. of Thrace, Xanthi, Greece.
[2]Asst., School of Engrg., Democritus Univ. of Thrace, Xanthi, Greece.

Note.—Discussion open until May 1, 1982. To extend the closing date one month, a written request must be filed with the Manager of Technical and Professional Publications, ASCE. Manuscript was submitted for review for possible publication on March 9, 1981. This paper is part of the Journal of the Irrigation and Drainage Division, Proceedings of the American Society of Civil Engineers, ©ASCE, Vol. 107, No. IR4, December, 1981. ISSN 0044-7978/81/0004-0411/$01.00.

in which δ = equivalent depth; σ = drain spacing; κ_1 and κ_2 = hydraulic conductivities of the pervious soil strata, respectively, above and below the plane through the drain axes; η = maximum height of the free-water surface above the drain axes level (total loss of hydraulic head to sustain the ground-water flow towards the drains); ϕ_1 = a function of the drain radius, given by the relation

$$\phi_1(\rho) = -\frac{1}{\pi} \ln \rho \quad \ldots\ldots\ldots\ldots\ldots\ldots\ldots\ldots\ldots\ldots\ldots\ldots\ldots\ldots (2)$$

in which ρ = the radius of the drain; and ϕ_2 = a function of the drain spacing which is given by the relations

$$\phi_2(\sigma) = \frac{1}{\pi}\left\{ \ln \frac{\sigma}{\pi} + \frac{1}{2} \sum_{n=1}^{\infty} \ln \frac{\left[(2n-1)^2 \frac{\sigma^2}{4} + 4\right]^2}{[(n-1)^2\sigma^2 + 4]\,(n^2\sigma^2 + 4)} \right\}; \quad \sigma \le \sigma_L \quad \ldots\ldots\ldots\ldots\ldots\ldots (3a)$$

$$\text{or} \quad \phi_2(\sigma) = \frac{1}{\pi}\left\{ -\ln \sqrt{2} + \sum_{n=1}^{\infty} \ln\left[1 - \frac{1}{2n^2\sigma^2}\right] + \frac{1}{2} \sum_{n=-\infty}^{\infty} \ln \frac{\left(n\sigma - \frac{\sqrt{2}}{2}\right)^2 + 4}{n^2\sigma^2 + 4} \right\} + \frac{(\sigma - \sqrt{2})^2}{8\sigma}; \quad \sigma > \sigma_L \quad \ldots\ldots\ldots\ldots\ldots\ldots (3b)$$

in which σ_L = a limiting value of σ which was found to be equal to 4.60.

The value of the function $\phi_1(\rho)$ can be determined easily. The function $\phi_2(\sigma)$ was computed with sufficient accuracy and a table has been prepared (3). Alternatively, for practical purposes, a graph has been constructed (3). The table can be stored in a computer memory and thus the determination of the equivalent depth for solving either Eq. 1*b* or an unsteady state drainage problem, where the notion of equivalent depth is utilized, becomes a rather easy task.

Simple Algebraic Equations for Function $\phi_2(\sigma)$.—A much simpler approach than that previously described for the determination of the equivalent depth would be the use of simple algebraic equations to approximate accurately the function $\phi_2(\sigma)$ given by the complicated relations of Eqs. 3*a* and 3*b*. Using a series of 100 values of $\phi_2(\sigma)$ for σ, ranging from 0.01–1000, the three curves described by the following equations were fitted to the given data by the least squares method: For σ ranging from 0.01–2.00

$$\phi_2'(\sigma) = 0.733 \log \sigma - 0.364 \quad \ldots\ldots\ldots\ldots\ldots\ldots\ldots\ldots\ldots\ldots\ldots\ldots (4a)$$

For σ ranging from 2.00–4.60

$$\phi_2'(\sigma) = 0.345\,(\log\sigma)^2 + 0.508\log\sigma - 0.326 \quad \ldots\ldots\ldots\ldots\ldots\ldots \quad (4b)$$

For σ greater than 4.60

$$\phi_2'(\sigma) = 0.125\,\sigma + \frac{0.160}{\sigma} - 0.443 \quad \ldots\ldots\ldots\ldots\ldots\ldots\ldots\ldots \quad (4c)$$

in which the prime was used to indicate the approximate value of $\phi_2(\sigma)$.

The error in computing the equivalent depth using the approximate values of the function ϕ_2 given by Eqs. 4, as compared with the "exact" values given by Eqs. 3, can be estimated as follows:

Differentiation of Eq. 1*a* with respect to ϕ_2 and rearrangement yields the relative error of δ due to using slightly different values of ϕ_2. Thus

$$\frac{\Delta\delta}{\delta} = -\frac{\Delta\phi_2}{\phi_1 + \phi_2} \quad \ldots\ldots\ldots\ldots\ldots\ldots\ldots\ldots\ldots\ldots\ldots\ldots \quad (5)$$

The largest relative error occurs for the minimum value of ϕ_1 which in turn

TABLE 1.—Relative Error in Computing Equivalent Depth

σ (1)	$\Delta\delta/\delta$, as a percent (2)	σ (3)	$\Delta\delta/\delta$, as a percent (4)
0.01	−0.08	3.60	−0.13
0.10	−0.10	4.60	0.12
0.50	−0.11	4.60	−0.67
1.00	−0.12	5.00	−0.40
1.10	−0.12	10.00	0.15
2.00	0.24	50.00	−0.01
2.00	−0.23	100.00	−0.01
2.20	0.09	200.00	−0.01
2.40	0.20	500.00	0.00
3.00	0.02	1000.00	0.00

occurs for the maximum possible value of ρ. The latter, designated by ρ_M, yields the maximum value of δ for a given value of σ. Table 1 indicates the upper limits of the error as a percentage of δ.

On the other hand, an estimation of the relative error in σ, resulting from a small error in δ, is obtained by differentiation of Eq. 1*b* with respect to δ and rearrangement. Thus, one obtains

$$\frac{\Delta\sigma}{\sigma} = \frac{1}{2}\left(1 - \frac{4\,\kappa_1\,\eta^2}{\sigma^2}\right)\frac{\Delta\delta}{\delta} \quad \ldots\ldots\ldots\ldots\ldots\ldots\ldots\ldots\ldots\ldots \quad (6)$$

The largest relative error occurring for $\eta \simeq 0$ is

$$\max\left(\frac{\Delta\sigma}{\sigma}\right) \simeq \frac{1}{2}\frac{\Delta\delta}{\delta} \quad \ldots\ldots\ldots\ldots\ldots\ldots\ldots\ldots\ldots\ldots\ldots\ldots \quad (7)$$

As can be confirmed from Table 1, the simple formulas of Eqs. 4*a*–4*c* approximate

the complicated relations of Eqs. 3*a* and 3*b* closely enough to yield an error in the value of the equivalent depth of less than 1%.

In a similar analysis (3) concerning the use of the formulas developed by Moody, the maximum relative error of equivalent depth was found to be in the order of 7%.

Summary and Conclusions

Based on a previous general and dimensionless treatment of the Hooghoudt equations for computing the equivalent depth and drain spacing, simple algebraic relations were developed for an easy and sufficiently accurate approximation of the function $\phi_2(\sigma)$. Thus, the task of computing the equivalent depth for solving steady or unsteady state drainage problems either by a desk calculator or on a digital computer becomes very simple, while the values computed suffer no appreciable loss of accuracy.

Appendix I.—References

1. Hooghoudt, S. B., "*Bijdragen tot de Kennis van Eenige Natuurkundige Grootheden van den Grond, 7, Algemeene Beschouwing van het Probleem van de Detailontwatering en de Infiltratie door Middel van Parallel Loopende Drains, Greppels, Slooten en Kanalen*," *Verslagen van Landbouwkundige Onderzoekingen*, No. 46 (14)B, The Hague, The Netherlands, 1940, pp. 515–707.
2. Moody, W. T., "Nonlinear Differential Equations of Drain Spacing," *Journal of the Irrigation and Drainage Division*, ASCE, Vol. 92, No. IR2, Proc. Paper 4835, June, 1966, pp. 1–9.
3. Sakkas, J. G., "Generalized Nomographic Solution of Hooghoudt Equations," *Journal of the Irrigation and Drainage Division*, ASCE, Vol. 101, No. IR1, Proc. Paper 11182, Mar., 1975, pp. 21–39.
4. Van Schilfgaarde, J., "Design of Tile Drainage for Falling Water Tables," *Journal of the Irrigation and Drainage Division*, ASCE, Vol. 89, No. IR2, Proc. Paper 3543, June, 1963, pp. 1–11.

Appendix II.—Notation

The following symbols are used in this note (all variables are dimensionless):

δ = equivalent depth;
η = maximum water-table height above drain-axes level;
κ_1 = hydraulic conductivity of the layer above drain-axes level;
κ_2 = hydraulic conductivity of the layer below drain-axes level;
ρ = radius of tile drains;
ρ_M = maximum realistic value of ρ for given value of σ;
σ = drain spacing;
σ_L = limiting value of σ determining application of Eq. 3*a* or 3*b*;
$\phi_1(\rho)$ = function of ρ (Eq. 2);
$\phi_2(\sigma)$ = function of σ (Eq. 3*a* or 3*b*);
$\phi_2'(\sigma)$ = function of σ approximating $\phi_2(\sigma)$ (Eqs. 4).

DISCUSSION

Note.—This paper is part of the Journal of the Irrigation and Drainage Division, Proceedings of the American Society of Civil Engineers, ©ASCE, Vol. 107, No. IR4, December, 1981. ISSN 0044-7978/81/0004-0417/$01.00.

Discussions

Discussions may be submitted on any Proceedings paper or technical note published in any *Journal* or on any paper presented at any Specialty Conference or other meeting, the *Proceedings* of which have been published by ASCE. Discussion of a paper/technical note is open to anyone who has significant comments or questions regarding the content of the paper/technical note. Discussions are accepted for a period of 4 months following the date of publication of a paper/technical note and they should be sent to the Manager of Technical and Professional Publications, ASCE, 345 East 47th Street, New York, N.Y. 10017. The discussion period may be extended by a written request from a discusser.

The original and three copies of the Discussion should be submitted on 8-1/2-in. (220-mm) by 11-in. (280-mm) white bond paper, typed double-spaced with wide margins. The length of a Discussion is restricted to two *Journal* pages (about four typewritten double-spaced pages of manuscript including figures and tables); the editors will delete matter extraneous to the subject under discussion. If a Discussion is over two pages long it will be returned for shortening. All Discussions will be reviewed by the editors and the Division's or Council's Publications Committees. In some cases, Discussions will be returned to discussers for rewriting, or they may be encouraged to submit a paper or technical note rather than a Discussion.

Standards for Discussions are the same as those for Proceedings Papers. A Discussion is subject to rejection if it contains matter readily found elsewhere, advocates special interests, is carelessly prepared, controverts established fact, is purely speculative, introduces personalities, or is foreign to the purposes of the Society. All Discussions should be written in the third person, and the discusser should use the term "the writer" when referring to himself. The author of the original paper/technical note is referred to as "the author."

Discussions have a specific format. The title of the original paper/technical note appears at the top of the first page with a superscript that corresponds to a footnote indicating the month, year, author(s), and number of the original paper/technical note. The discusser's full name should be indicated below the title (see Discussions herein as an example) together with his ASCE membership grade (if applicable).

The discusser's title, company affiliation, and business address should appear on the first page of the manuscript, along with the *Proceedings* paper number of the original paper/technical note, the date and name of the *Journal* in which it appeared, and the original author's name.

Note that the discusser's identification footnote should follow consecutively from the original paper/technical note. If the paper/technical note under discussion contained footnote numbers 1 and 2, the first Discussion would begin with footnote 3, and subsequent Discussions would continue in sequence.

Figures supplied by the discusser should be designated by letters, starting with A. This also applies separately to tables and references. In referring to a figure, table, or reference that appeared in the original paper/technical note use the same number used in the original.

It is suggested that potential discussers request a copy of the *ASCE Authors' Guide to the Publications of ASCE* for more detailed information on preparation and submission of manuscripts.

Expanded Polystyrene Spheres as Evaporation Suppressors[a]

Discussion by A. F. Thoma[4]

The authors have presented a description of experiments applying expanded polystyrene beads to reduce evaporation. When adopting new material and methods, indoor and outdoor tests are very useful, not solely to prove the practical application and its economic advance but for the possibility of comparison and for solving theoretical problems, if any. In this respect, the writer would like to expand the completion on the critical considerations.

Comparison of Evaporation Control Percentages.—According to the authors, "A combined cover suppressed evaporation by 70.2% . . . and polystyrene covers respectively" (p. 168). A more detailed comparison of these figures is noteworthy, as far as the contact surface ratios of the different cover materials are concerned. To make more perceptible the evaporation reduction ratios, the writer has taken the liberty of drawing up Fig. 8, on which the cross sections and the view of the used cover material are shown.

It is assumed that the contact surface between the polystyrene spheres and the water (Fig. 8) can be expressed as

$$f_1 = 0.422\,F \quad \ldots\ldots\ldots\

2. If the specific gravity is higher the sphere will submerge deeper in the water, consequently, "D'" will be larger and so the reduction ratio will increase.

Different Temperature Elevations of Water.—The tested polystyrene spheres of 2 mm–8 mm diameter is a byproduct whose material has considerable insulation features. This is one of the reasons for the temperature increase. On the other hand, one should take into consideration the fact that, during evaporation, the

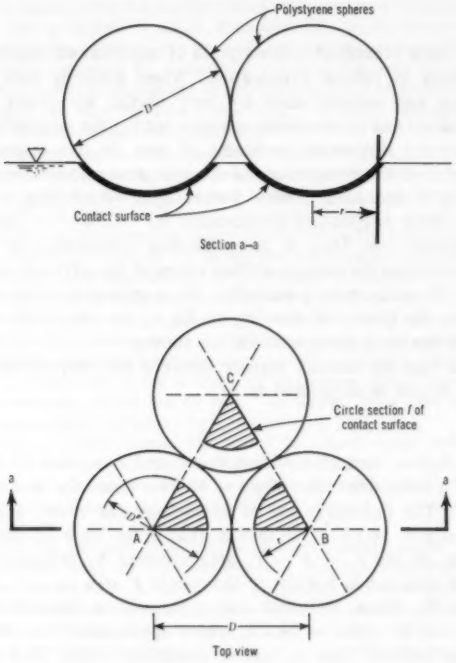

FIG. 8.—Cross Sections and View of Used Cover Material

vapor molecules leaving the water surface transfer certain heat, Q_e, the so called "evaporation heat" i.e.

$$Q_e \cong 594.9 - 0.51\,T_w \quad \ldots\ldots\ldots\

T_w, plotted against the depth of uncovered water $z_{(-)}$. The dotted line, marked *B* on Fig. 9, shows the same diagram for water covered with polystyrene spheres.

Between the two lines are the kind of differences. In one respect as the evaporation rate is reduced by the cover material, the heat loss of water is lower, consequently the surface temperature will be higher as

$$\Delta t_e = \Delta t'_e - \Delta t''_e \quad \ldots\ldots\ldots\

Technical Papers

Original papers should be submitted in triplicate to the Manager of Technical and Professional Publications, ASCE, 345 East 47th Street, New York, N.Y. 10017. Authors must indicate the Technical Division or Council, Technical Committee, Subcommittee, and Task Committee (if any) to which the paper should be referred. Those who are planning to submit material will expedite the review and publication procedures by complying with the following basic requirements:

1. Titles must have a length not exceeding 50 characters and spaces.

2. The manuscript (an original ribbon copy and two duplicate copies) should be double-spaced on one side of 8-1/2-in. (220-mm) by 11-in. (280-mm) paper. Three copies of all figures and tables must be included.

3. Generally, the maximum length of a paper is 10,000 word-equivalents. As an *approximation*, each full manuscript page of text, tables or figures is the equivalent of 300 words. If a particular subject cannot be adequately presented within the 10,000-word limit, the paper should be accompanied by a rationale for the overlength. This will permit rapid review and approval by the Division or Council Publications and Executive Committees and the Society's Committee on Publications. Valuable contributions to the Society's publications are not intended to be discouraged by this procedure.

4. The author's full name, Society membership grade, and a footnote stating present employment must appear on the first page of the paper. Authors need not be Society members.

5. All mathematics must be typewritten and special symbols must be identified properly. The letter symbols used should be defined where they first appear, in figures, tables, or text, and arranged alphabetically in an appendix at the end of the paper titled Appendix.—Notation.

6. Standard definitions and symbols should be used. Reference should be made to the lists published by the American National Standards Institute and to the *Authors' Guide to the Publications of ASCE*.

7. Figures should be drawn in black ink, at a size that, with a 50% reduction, would have a published width in the *Journals* of from 3 in. (76 mm) to 4-1/2 in. (110 mm). The lettering must be legible at the reduced size. Photographs should be submitted as glossy prints. Explanations and descriptions must be placed in text rather than within the figure.

8. Tables should be typed (an original ribbon copy and two duplicates) on one side of 8-1/2-in. (220-mm) by 11-in. (280-mm) paper. An explanation of each table must appear in the text.

9. References cited in text should be arranged in alphabetical order in an appendix at the end of the paper, or preceding the Appendix.—Notation, as an Appendix.—References.

10. A list of key words and an information retrieval abstract of 175 words should be provided with each paper.

11. A summary of approximately 40 words must accompany the paper.

12. A set of conclusions must end the paper.

13. Dual units, i.e., U.S. Customary followed by SI (International System) units in parentheses, should be used throughout the paper.

14. A practical applications section should be included also, if appropriate.